



MID-AMERICA TRANSPORTATION CENTER

Report # MATC-UNL: 226

Final Report



Study of RF Propagation Characteristics for Wireless Sensor Networks in Railroad Environments

Hamid Sharif, Ph.D.

Henson Professor

Computer and Electronics Engineering

University of Nebraska-Lincoln

Michael Hempel, Ph.D.



2010

A Cooperative Research Project sponsored by the
U.S. Department of Transportation Research and
Innovative Technology Administration

The contents of this report reflect the views of the authors, who are responsible for the facts and the accuracy of the information presented herein. This document is disseminated under the sponsorship of the Department of Transportation University Transportation Centers Program, in the interest of information exchange.
The U.S. Government assumes no liability for the contents or use thereof.

MATC

**Study of RF Propagation Characteristics for Wireless Sensor Networks
in Railroad Environments**

Hamid Sharif
Henson Professor
Department of Computer and Electronics
Engineering
University of Nebraska-Lincoln

Michael Hempel
Research Assistant Professor
Department of Computer and Electronics
Engineering
University of Nebraska-Lincoln

A Report on Research Sponsored By

Mid-America Transportation Center

University of Nebraska-Lincoln

June 2010

Technical Report Documentation Page

1. Report No. 25-1121-0001-226	2.	3. Recipient's Accession No.	
4. Title and Subtitle Study of RF Propagation Characteristics for Wireless Sensor Networks in Railroad Environments		5. Report Date 07/06/2010	
		6.	
7. Author(s) Hamid Sharif Michael Hempel		8. Performing Organization Report No. MATC TRB RiP No. 22318	
9. Performing Organization Name and Address Advanced Telecommunications Engineering Laboratory Dept. Of Computer and Electronics Engineering, PKI 304, 1110 South 67th Street, Omaha, NE 68182		10. Project/Task/Work Unit No.	
		11. Contract © or Grant (G) No.	
12. Sponsoring Organization Name and Address Mid-America Transportation Center U.S. Department of Transportation Region VII University Transportation Center University of Nebraska-Lincoln 2200 Vine Street 262 Whittier Building Lincoln, Nebraska 68583-0851		13. Type of Report and Period Covered Final Research Report	
		14. Sponsoring Agency Code	
15. Supplementary Notes			
16. Abstract (Limit: 200 words)			
<p>The freight railroad industry in North America is exerting efforts to leverage Wireless Sensor Networks to monitor systems and components on railcars. This allows fault detection and accident prevention even while a train is moving.</p> <p>Railcars, constructed mostly of ferrous materials such as steel, are expected to severely impact signal propagation. To better understand this effect we first evaluated the signal characteristics when sensor nodes are placed in various locations around railcars. We used EM-Field modeling and evaluation techniques to obtain these results and found that node placement selection is critical for the node's communication distance.</p> <p>As a second research area we therefore aimed at understanding the protocol requirements and limitations of current WSN technologies. Based on the results of our study we found ZigBee to be inadequate for freight WSNs and developed a solution that remedies the problems we observed. Our evaluation of this new multi-tier approach shows a significant performance and network lifetime gain, making freight train wireless sensor networks feasible.</p>			
17. Document Analysis/Descriptors		18. Availability Statement	
19. Security Class (this report)	20. Security Class (this page)	21. No. of Pages 79	22. Price

Table of Contents

CHAPTER 1	INTRODUCTION.....	1
CHAPTER 2	RESEARCH PHASE 1: PROPAGATION STUDIES FOR WIRELESS SENSOR NODES	3
2.1	Introduction to Propagation Analysis	3
2.2	Overview of CST Microwave Studio	5
2.3	Modeling of freight railcars	8
2.3.1	A boxcar and its 3D model	8
2.3.2	A tanker car and its 3D model	10
2.3.3	A flat car and its 3D model.....	12
2.3.4	A hopper car and its 3D model.....	13
2.4	Showcasing signal characteristics on and around railcars for various configurations.....	15
2.4.1	The roof-mounted antenna simulation.....	17
2.4.2	The side-mounted antenna simulation.....	20
2.5	Conclusions and Impact on wireless sensor networks onboard freight trains	33
CHAPTER 3	RESEARCH PHASE 2: WIRELESS SENSOR NETWORKS PROTOCOL STUDY TO EVALUATE PERFORMANCE CAPABILITIES	34
3.1	Methodology for WSN protocol study	34
3.2	Evaluated Wireless Sensor Network Platforms	35
3.3	Qualnet Simulator	36
3.4	OPNET Simulator.....	40
3.5	NS-2 Simulator	43
CHAPTER 4	PROPOSED SOLUTION: MULTI-LAYER MULTI-HOP NETWORKS	47
4.1	Description.....	47
4.2	Network Simulations	49
4.2.1	General Simulation Scenario.....	49
4.2.2	QualNet.....	49
4.2.3	OPNET	52
4.2.4	NS-2.....	53
4.3	Energy Analysis of the proposed multi-tier multi-hop scheme	56
CHAPTER 5	PUBLICATIONS.....	61

CHAPTER 6 SUMMARY62
Appendix A: Additional Results from EM-Field Study of RF Propagation Characteristics...66

List of Figures

Figure 2.1 Train undercarriage and tracks up close.....	4
Figure 2.2 CST Microwave Studio modeling and simulation environment.....	6
Figure 2.3 Boxcar photograph	9
Figure 2.4 Boxcar model in CST Microwave Studio	9
Figure 2.5 Tank Car photographs	11
Figure 2.6 Tank car model in CST Microwave Studio.....	11
Figure 2.7 Flat Car photographs	12
Figure 2.8 Flat car model in CST Microwave Studio.....	13
Figure 2.9 Hopper Car photographs.....	14
Figure 2.10 Hopper car model in CST Microwave Studio	15
Figure 2.11 The monopole antenna and its radiation pattern	17
Figure 2.12 Scenario 1-Roof mounted antenna on boxcar: Placement.....	18
Figure 2.13 Scenario 1-Roof mounted antenna on boxcar: Farfield pattern	19
Figure 2.14 Scenario 1-Roof mounted antenna on boxcar: E-Field Visualization.....	20
Figure 2.15 Scenario 2-Side mounted antenna on boxcar: Placement	21
Figure 2.16 Scenario 2-Side mounted antenna on boxcar: Farfield Pattern	22
Figure 2.17 Scenario 2-Side mounted antenna on boxcar : E-Field Visualization.....	22
Figure 2.18 Scenario 3-Undercarriage mounted antenna on boxcar: Placement.....	23
Figure 2.19 Scenario 3-Undercarriage mounted antenna on boxcar: Farfield Pattern	24
Figure 2.20 Scenario 3-Undercarriage mounted antenna on boxcar: E-Field Visualization	25
Figure 2.21 Scenario 3-Undercarriage mounted antenna on boxcar: Power Flow Analysis	26
Figure 2.22 Scenario 4-Roof mounted antenna on boxcar passing train: Placement	27

Figure 2.23 Scenario 4-Roof mounted antenna on boxcar passing train: Farfield Pattern	28
Figure 2.24 Scenario 4-Roof mounted antenna on boxcar passing train: E-Field Visualization..	29
Figure 2.25 Scenario 5-Roof mounted antenna on boxcar in train segment: Placement.....	30
Figure 2.26 Scenario 5-Roof mounted antenna on boxcar in train segment: Farfield Pattern	31
Figure 2.27 Scenario 5-Roof mounted antenna on boxcar in train segment: E-Field Visualization	32
Figure 3.1 Evaluated Sensor Platforms.....	35
Figure 3.2 Simulation Setup in QualNet.....	37
Figure 3.3 Beacon Synchronization.....	38
Figure 3.4 Average No. of Beacons sent (left) and Average No. of data packets forwarded (right) in our QualNet simulations	40
Figure 3.5 Simulation topology for OPNET.....	41
Figure 3.6 End-to-end delay and throughput results collected from OPNET simulator	42
Figure 3.7 Number of beacon frames sent, received, and dropped in ns-2	44
Figure 3.8 Number of data packets sent and received in ns-2	45
Figure 4.1 Proposed Multi-layer Multi-hop network strategy	48
Figure 4.2 Multi-layer multi-hop wireless sensor network in QualNet	49
Figure 4.3 Number of beacon frames sent and received in QualNet	50
Figure 4.4 Number of data packets sent and received in QualNet	51
Figure 4.5 Multi-layer multi-hop wireless sensor network in OPNET.....	52
Figure 4.6 Number of beacon frames sent, received, and dropped in ns-2	54
Figure 4.7 Number of data packets sent and received in ns-2	54
Figure 4.8 Number of packets delivered at destination in each second.....	55

Figure 4.9 Energy consumption per node comparison	59
Figure 4.10 Network Lifetime comparison between traditional scheme and multi-tier networking	60
Figure A.1. Tanker car: roof-mounted antenna.....	67
Figure A.2. Flat car: side-mounted antenna.....	68
Figure A.3. Tank car: side-mounted antenna.....	69
Figure A.4. Hopper car: side-mounted antenna.....	70
Figure A.5. Flat car: undercarriage-mounted antenna.....	71
Figure A.6. Tank car: undercarriage-mounted antenna.....	72
Figure A.7. Hopper car: undercarriage-mounted antenna.....	73
Figure A.8. Flat car: passing train.....	74
Figure A.9. Tanker car: passing train.....	75
Figure A.10. Hopper car: passing train.....	76
Figure A.11. Flat car: train segment.....	77
Figure A.12. Tanker car: train segment.....	78
Figure A.13. Hopper car: train segment.....	79

List of Tables

Table 2.1 Boxcar 3D Model Statistics	10
Table 2.2 Tank Car 3D Model Statistics.....	11
Table 2.3 Flat Car 3D Model Statistics.....	13
Table 2.4 Hopper Car 3D Model Statistics.....	15
Table 4.1 Battery Types and their average energy storage capacities	57
Table 4.2 Zigbee and Wi-Fi Chipset comparison for power consumption.....	58

Acknowledgements

We would like to thank Union Pacific for their generous support of our research throughout the entire project. UP provided technical expertise in railcar monitoring, sensor platforms for lab testing, and an open ear for all of our questions. We will always cherish the close collaboration of our team here at TEL with the people at Union Pacific.

Abstract

The freight railroad industry in North America is exerting efforts to leverage Wireless Sensor Networks to monitor systems and components on railcars. This allows fault detection and accident prevention even while a train is moving.

Railcars, constructed mostly of ferrous materials such as steel, are expected to severely impact signal propagation. To better understand this effect we first evaluated the signal characteristics when sensor nodes are placed in various locations around railcars. We used EM-Field modeling and evaluation techniques to obtain these results and found that node placement selection is critical for the node's communication distance.

As a second research area we therefore aimed at understanding the protocol requirements and limitations of current WSN technologies. Based on the results of our study we found ZigBee to be inadequate for freight WSNs and developed a solution that remedies the problems we observed. Our evaluation of this new multi-tier approach shows a significant performance and network lifetime gain, making freight train wireless sensor networks feasible.

Executive Summary

This project focused on studying the characteristics of Wireless Sensor Networks onboard freight trains. In North America freight railroad companies are searching for ways to improve their monitoring capabilities and the fault detection of individual railcars. Small battery operated wireless sensor nodes can easily be installed onboard freight railcars to monitor a variety of systems from wheel imbalances and brake failures to refrigerator units, boxcar doors and much more.

This study first evaluated the propagation characteristics at the physical layer of wireless sensor nodes deployed onboard railcars and found that placement of these nodes significantly impacts the radio wave propagation characteristics. In addition to placement, the effectiveness of the nodes is further complicated by the materials used in railcar construction and their design. This in turn drastically impacts the requirements upon the wireless communication protocols at the MAC and Routing layers.

In our second research effort for this project we studied the performance of ZigBee, a communication protocol stack commonly used in traditional wireless sensor networks. This protocol was found to be inadequate for the requirements placed upon freight train wireless sensor networks. We therefore proposed an alternative method using a multi-tiered approach that leverages a long-distance communication technology added to the wireless sensors, and studied its performance in an effort to overcome the limitations of ZigBee for freight car WSNs.

The proposed solution has been shown in our simulation study to be very promising in overcoming the observed problems and we found that our design provides significant performance improvements over the traditional approach, as well as significantly improved energy efficiency and network lifetime.

Chapter 1 Introduction

The University of Nebraska-Lincoln's [1] Advanced Telecommunications Engineering Laboratory (TEL) [2] has a long-standing tradition of close collaborations with Union Pacific Railroad [3] and other North American freight railroad companies. For the past several years the railroad industry's focus has been on making their operations safer and more secure by protecting and monitoring transported goods, equipment, and infrastructure.

TEL has started a collaborative project with Union Pacific sponsored by the Mid-America Transportation Center (MATC) [4] at the University of Nebraska-Lincoln. The intention of this project is to study the characteristics of Wireless Sensor Networks (WSN) deployed on freight rail cars in a collaborative effort to develop a WSN-based solution for continuous real-time monitoring and reporting. A solution for this problem represents a major contribution since, to the best of our knowledge, none have been proposed thus far. The envisioned end system will be able to observe operational conditions such as brake status on rail cars, the status of cargo doors, temperatures inside air-conditioned rail cars for transporting perishable goods, the track status, and many other parameters that are vital for providing a safe and secure transportation environment.

Even before this project started the TEL lab had established a dialog with Union Pacific about their experiences with and requirements for using WSN technology in their operations. All encountered problems were collected and prioritized for subsequent in-depth studies. The most important problems reported, and the focus of our study with MATC and Union Pacific, are the unreliable route formation that results from the nature of a freight train that requires a very long chain topology. This type of topology typically has a hop count of 100 or more hops on a freight train. Another important factor is the uncertainty of RF propagation and link characteristics that

results from the placement of WSN sensor nodes and the influence of the rail car construction and materials.

Chapter 2 Research Phase 1: Propagation Studies for Wireless Sensor Nodes onboard freight railcars

2.1 Introduction to Propagation Analysis

For a comprehensive evaluation and understanding of the implications of installing Wireless Sensor Networks onboard freight trains we first need to analyze the RF signal's propagation characteristics. We need to understand the communication distance of individual nodes as well as to evaluate how and where to install the nodes and antennas. Placement of these devices must be close to the monitored event sources (such as wheels, brakes, boxcar doors, refrigerator units, etc.) without impeding the signal path with obstacles, low ground clearance, and other impairments. We also need to analyze optimization strategies for node placement to minimize system deployment and maintenance cost, as well as possible beneficial or required alterations to railcar construction.

RF signals are electromagnetic waves propagating through a medium: such as air radiating from a transmitter and travelling in all directions. Electromagnetic waves emanate from antenna structures as a result of an oscillating electric field that in turn generates an oscillating magnetic field, as governed by Maxwell's equations. This waveform travels at the speed of light through the carrier medium.

Obstacles such as buildings, cars, trees, or even the ground can impact signal propagation paths. Surfaces can scatter signals, an effect that is especially severe around trees, and obstacle edges can diffract signal paths. Radio waves can also be severely impacted by specific materials in the propagation area. Especially ferrous materials, such as steel and iron, can drastically alter signal propagation characteristics, communication distances, link quality, and many other factors.

With that in mind, it is important to realize that both railcars and railroad tracks are comprised of a large amount of ferrous materials, as shown in Figure 2.1. Radio waves induce currents in these materials, dissipating some of their energy in the process. These induced currents then can generate EM fields that radiate from them and alter the propagation characteristics of the original RF signal.



Figure 2.1 Train undercarriage and tracks up close

To better understand the impact of such materials and how they influence possible placement of sensor nodes onboard freight railcars, we first conducted a comprehensive simulation study that involved a specialized simulation package for EM-Field simulations: Microwave Studio by Computer Simulation Technology, Inc. (CST) [5].

2.2 Overview of CST Microwave Studio

Microwave Studio is a simulation software package designed to evaluate structures for their EM characteristics. One example application that this package is oftentimes used for is the evaluation of antenna radiation patterns during the design process of antennas—such as horn feeds for parabolic dish antennas, patch antennas, and smart antenna arrays. This software also allows us to evaluate the interaction between electronic circuits and radio waves; basically, it will simulate the interaction and interrelation between EM fields and structures. To do so, users either leverage the built-in 3D modeling environment or 3D object importer and its support for most common 3D file formats. The user assigns material properties to each individual component to fully represent the 3D object or objects and their properties. Assigning these properties is critical to the entire simulation and evaluation process. Air, for example, has drastically different EM properties than steel.

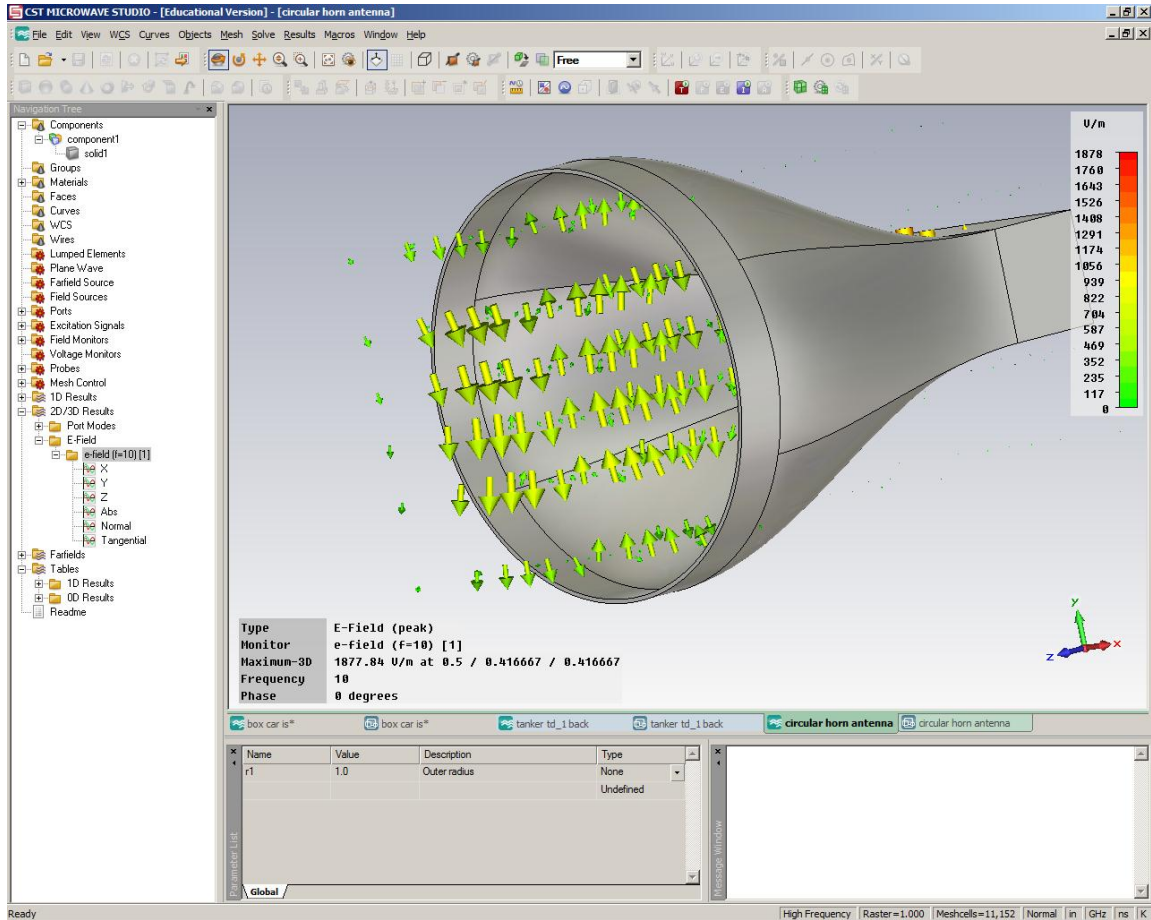


Figure 2.2 CST Microwave Studio modeling and simulation environment

The analysis of the modeled environment is then performed using one of the numerous system solvers available in CST Microwave Studio. These solvers include the following:

- Time-Domain Solver
- Frequency-Domain Solver
- Integral Equation Solver
- Eigenmode Solver
- Multilayer Solver
- Asymptotic Solver

Other solvers for related CST simulation tasks are:

- Microstripes Solver
- Cable Harness Solver
- Printed Circuit Boards Solver
- Static Bundle and Low-Frequency Bundle Solvers
- Tracking Solver for particle simulations
- Wakefield Solver for particle simulations
- Particle-in-Cell Solver
- Thermal Solver
- Structural Mechanics Solver
- Circuit Simulator

With such a vast array of solvers available to the end user the CST simulation suite of products can be applied to a very wide range of analysis and evaluation applications. For our research purposes we have licensed the time-domain and integral equation solvers.

Unlike frequency-domain solvers, which work best with electrically small structures such as circuit elements and printed circuit boards, time-domain solvers for EM-Field analysis are well-suited for the simulation of electrically large structures, such as cars, airplanes, buildings, and railcars. Time-domain solvers perform a transient analysis of the EM-Field, indicating the ways in which the E and H fields propagate through the simulated space over time. Time-domain solvers are also well-suited for the analysis of a large frequency range.

Integral equation solvers express Maxwell's equations as an integral. This allows the application of numerical evaluations particularly well-suited for mesh-defined models in the EM

simulation. Integral equation solvers are also more efficient in the use of computational resources such as system memory during their processing. This allows us to use a higher resolution mesh that in turn provides higher accuracy for the computed results.

With these two solvers we are able to compute EM field patterns and material interactions in spatially large structures, such as train segments comprised of multiple railcars.

2.3 Modeling of freight railcars

The first step for our EM analysis was to generate models of different railcars as used by freight railroad companies in North America. We chose to model the following car types: a boxcar, a tanker car, a flat car and a hopper car.

These four different railcar types represent the majority of types used by the freight railroad companies in North America. Other railcar types can be modeled if there is a particular need for their analysis. The following sections describe the available railcar types and models in more detail.

2.3.1 A boxcar and its 3D model

Boxcars are typically used to transport crated goods, or goods that are palletized for easy loading and unloading. It is a covered structure that typically features two sliding loading doors, one of each side, approximately centered along the long axis of the boxcar.



Figure 2.3 Boxcar photograph (© about.com)

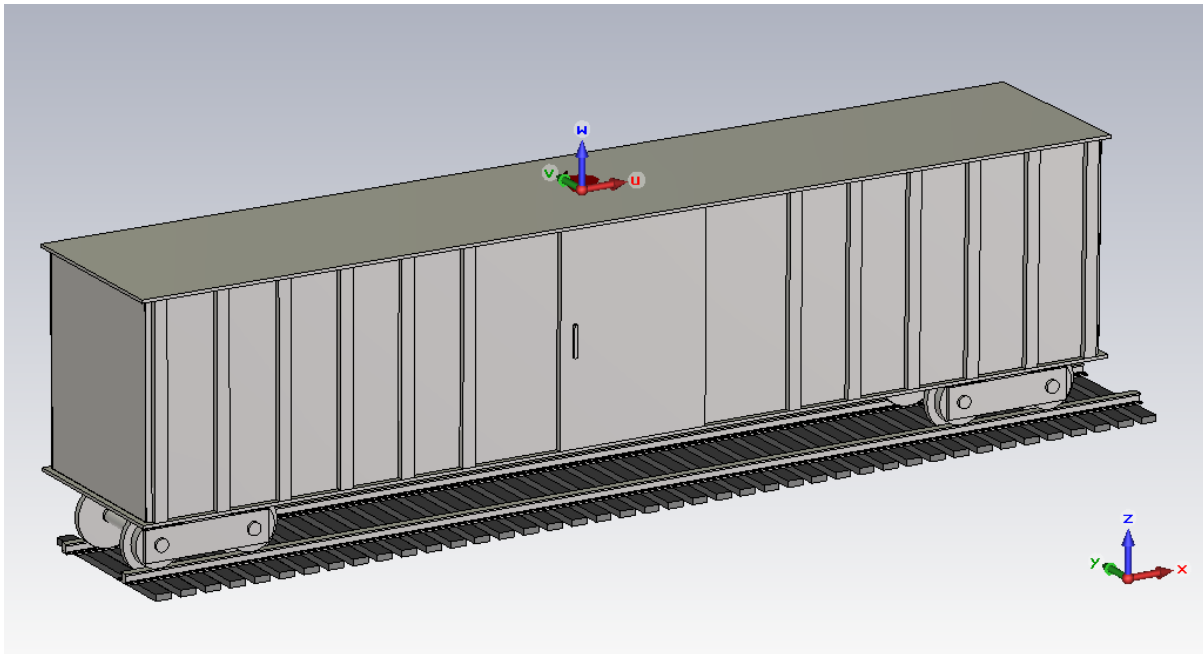


Figure 2.4 Boxcar model in CST Microwave Studio

Table 2.1 Boxcar 3D Model Statistics

Outside Length	15.8 m	51.84 ft
Inside Length	15.78 m	51.77 ft
Outside Width	2.8 m	9.18 ft
Inside Width	2.78 m	9.12 ft
Height (including undercarriage)	4.4 m	14.43 ft
Height (excluding undercarriage)	3.35 m	11 ft
Inside Volume	144.76 m ³	5112.35 cu ft or approx. 38243 gallons

2.3.2 A tanker car and its 3D model

Tanker cars are used to transport liquid and gaseous goods, such as petroleum, milk, and liquid hydrogen. To prevent the transported goods from reacting with the tank car's outer structure, the inside of the container is typically lined with an insulating material such as glass.





Figure 2.5 Tank Car photographs (Wikimedia public domain images)

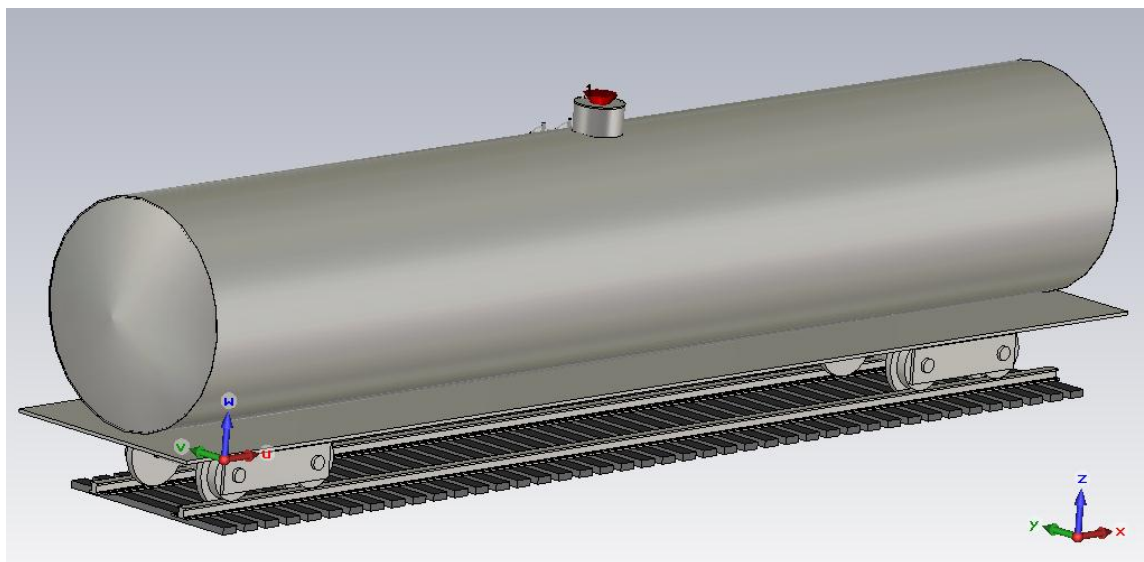


Figure 2.6 Tank car model in CST Microwave Studio

Table 2.2 Tank Car 3D Model Statistics

Outside Length	18.2 m	59.75 ft
Inside Length	17.4 m	57.12 ft
Outside Width	3.24 m	10.63 ft
Inside Width	3.19 m	10.47 ft
Height (including undercarriage)	4.72 m	15.48 ft
Height (excluding undercarriage)	3.72 m	12.2 ft
Inside Volume	139.15 m ³	4913.88 cu ft or approx. 36758 gallons

2.3.3 A flat car and its 3D model

Flat Cars are used to transport mostly freight containers that are loaded onto the flat bed provided by this railcar type. Other uses of flat cars include the transport of lumber, pipes, and similar goods.



Figure 2.7 Flat Car photographs (Wikimedia public domain images)

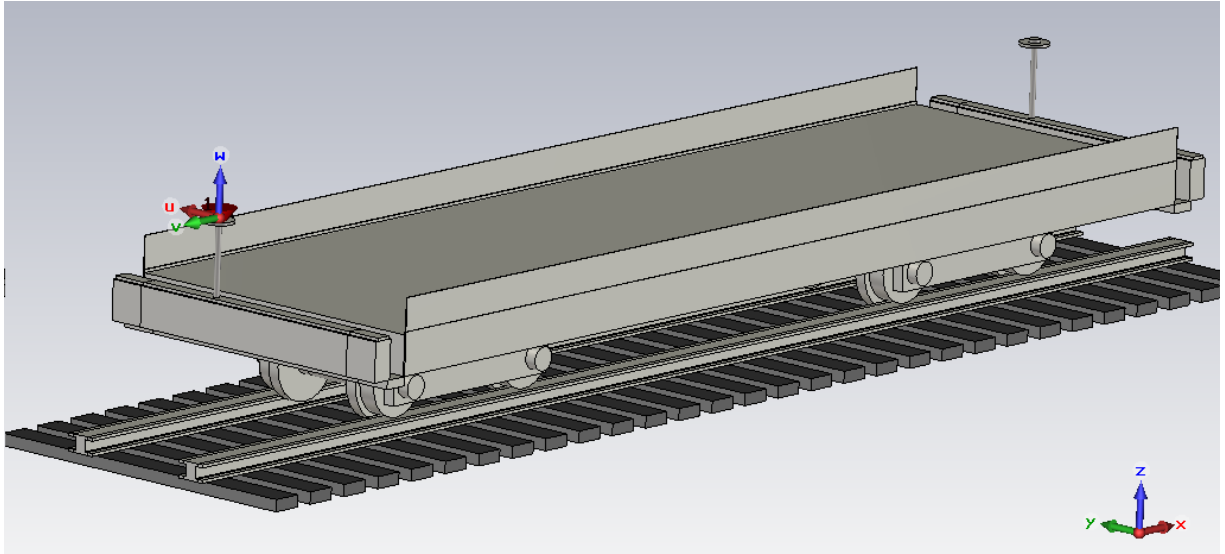


Figure 2.8 Flat car model in CST Microwave Studio

Table 2.3 Flat Car 3D Model Statistics

Outside Length	10.14 m	33.25 ft
Outside Width	2.82 m	9.25 ft
Height (including undercarriage)	1.71 m	5.6 ft
Height (excluding undercarriage)	0.99 m	3.25 ft
Area of Bed	26.12 m ³	281.1 sq ft

2.3.4 A hopper car and its 3D model

Finally, hopper cars are used to transport predominantly coal, but also grain, gravel, and other such materials. They are typically loaded from the top, but unloaded through chutes in the bottom of the railcar.



Figure 2.9 Hopper Car photographs

Note: These are public domain images. Top row: Greg Goebel, bottom row: flickr.com

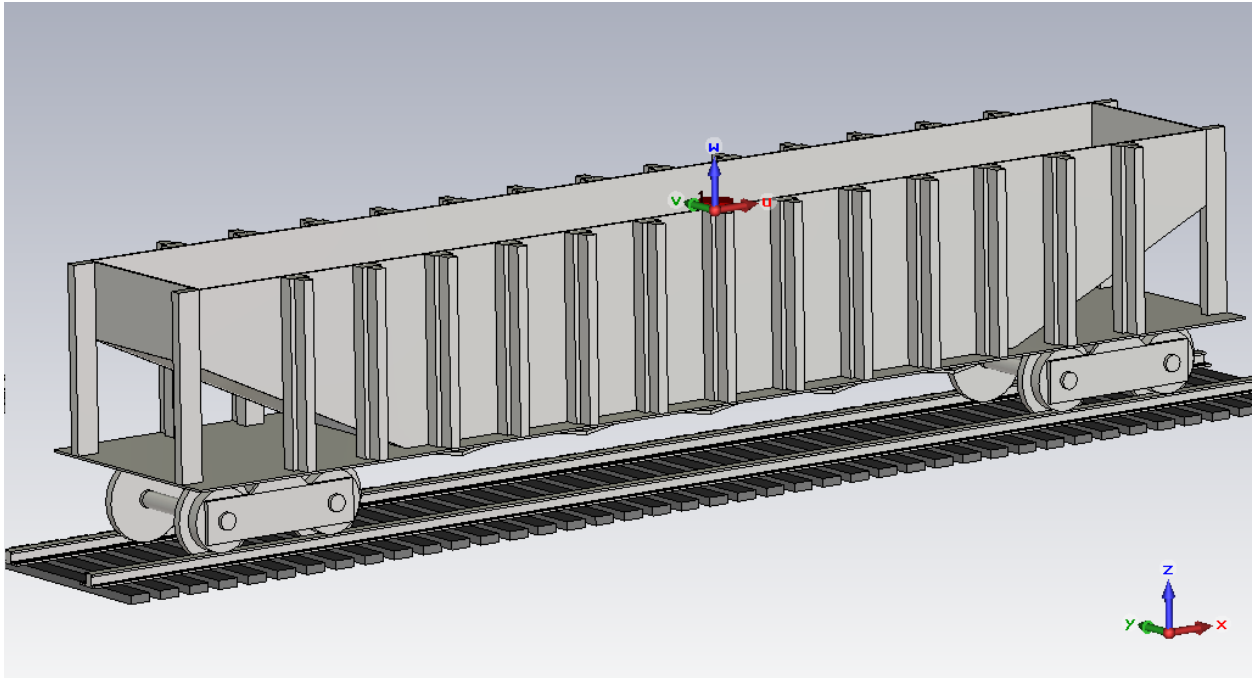


Figure 2.10 Hopper car model in CST Microwave Studio

Table 2.4 Hopper Car 3D Model Statistics

Outside Length	14.73 m	48.32 ft
Inside Length (Top)	14.15 m	46.42 ft
Inside Length (Bottom)	8.36 m	27.43 ft
Outside Width	2.86 m	9.38 ft
Inside Width	2.13 m	7 ft
Height (including undercarriage)	3.01 m	9.9 ft
Height (excluding undercarriage)	2.01 m	6.6 ft
Inside Volume	52.42 m ³	1851.3 cu ft or approx. 13848 gallons

2.4 Showcasing signal characteristics on and around railcars for various configurations

With the models for the railcars available we could finally commence our evaluation of the signal propagation characteristics on and around railcars. The results presented below focus on the boxcar model we created; appendix A will show the results corresponding with the other railcar types we modeled and evaluated.

Of particular importance to us in these tests was the placement of the sensor node and the resulting signal propagation. We used the EM simulations to gain insight into the distribution of signal strength at different locations around the evaluated railcar. This provides us information about the expected link quality if a sensor node was placed at this location and receives the transmission emanating from the source node. By placing the transmitting sensor at different locations around the railcar we could also evaluate the impact of both the railcar construction materials and the shape.

2.4.1 The roof-mounted antenna simulation

This effect of materials and railcar structure is highlighted by the first simulation we performed, which was for a boxcar with an antenna mounted centered on top of the boxcar's roof.

For all of our simulations we utilized a monopole antenna tuned for the 2.4 GHz frequency band typically used by wireless sensor network transceivers. ZigBee [6] is an example of a wireless communication protocol that is used in WSNs and is implemented in many common transceiver chipsets. ZigBee is based on IEEE 802.15.4 [7] and provides power-efficient communication over medium distances with data rates up to 250 kbps. The following two figures show the used monopole antenna on the left and its unobstructed farfield antenna pattern on the right.

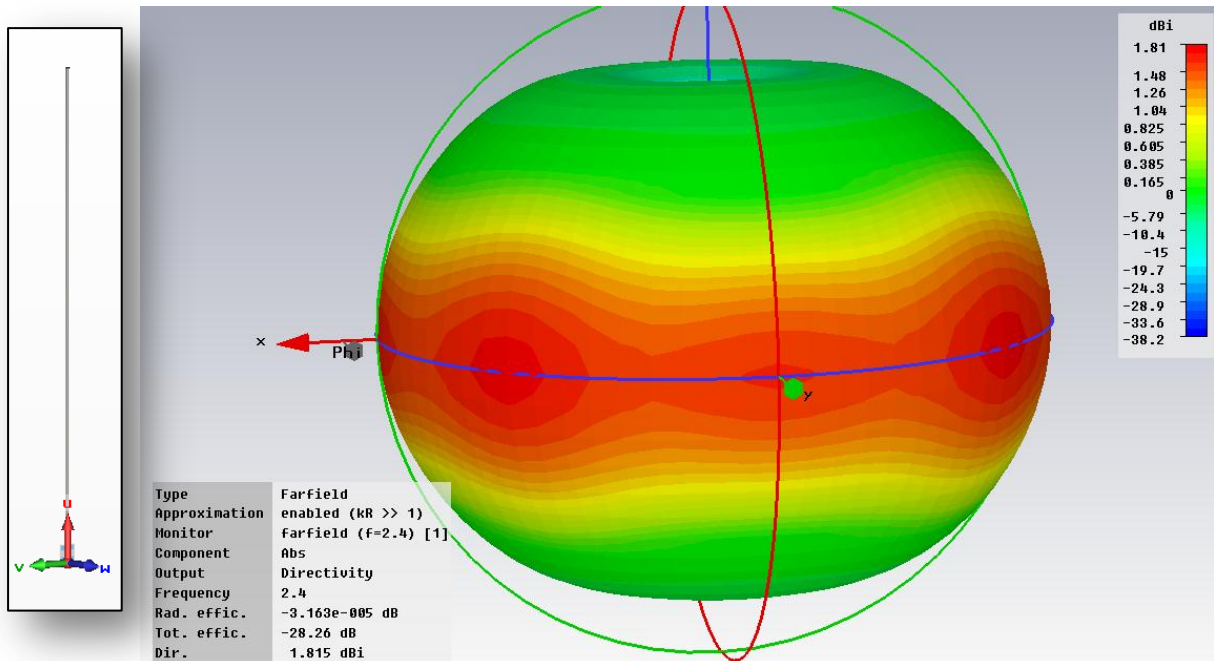


Figure 2.11 The monopole antenna and its radiation pattern

The following figure shows the placement of the monopole antenna on top of the boxcar with the insert highlighting the area.

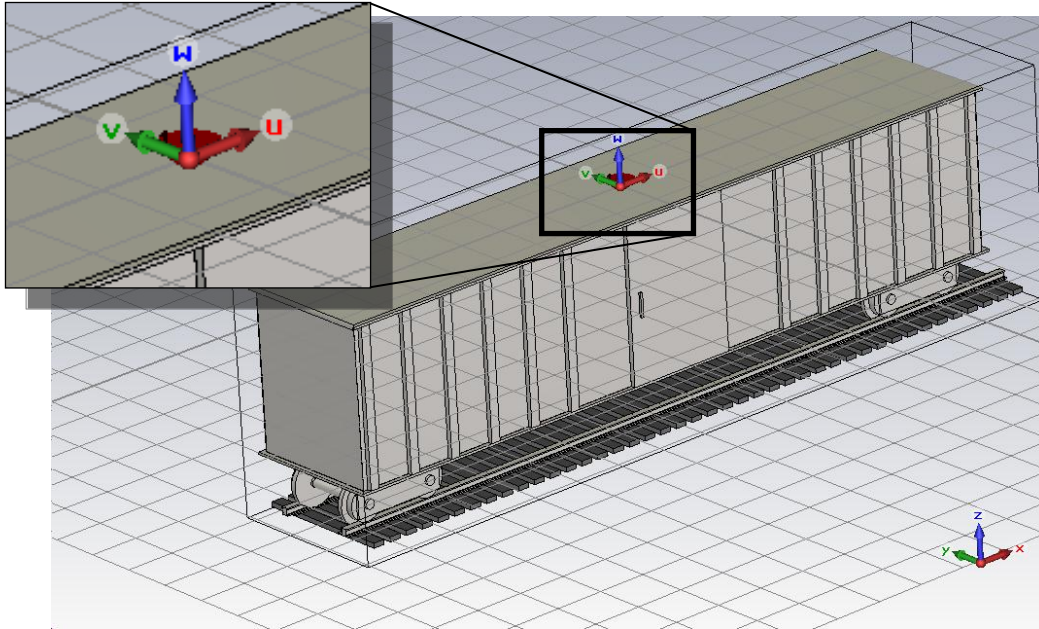


Figure 2.12 Scenario 1-Roof mounted antenna on boxcar: Placement

The following figure shows the resulting far-field antenna pattern that is determined by the simulation run. As we can see, the antenna pattern approximates a donut flattened at the bottom. This flattening is a direct result of the proximity of the antenna to the steel roof structure of the boxcar. Acting as an RF shield, the steel roof does not allow significant amounts of energy to radiate into the lower hemisphere and instead this energy is redirected upwards. This redirection generates the donut shape of the farfield pattern. It is also responsible for the band of red which indicates the direction of the strongest signals in the pattern. With an unobstructed monopole this band is expected to be in the horizontal plane. With such a pattern, the greatest

amount of energy would radiate directly away from the upright monopole antenna in a horizontal direction.

However, because of the energy redirected by the roof, this band is shifted upwards out of the horizontal plane. The maximum amount of radiated energy is now found at a slight upwards angle from the antenna; this angle is about 12 degrees in our simulations. It changes significantly with small increases in spacing between the roof and the antenna. The farther the antenna is raised above the roof, the closer this angle is to zero degrees and the original unobstructed monopole antenna.

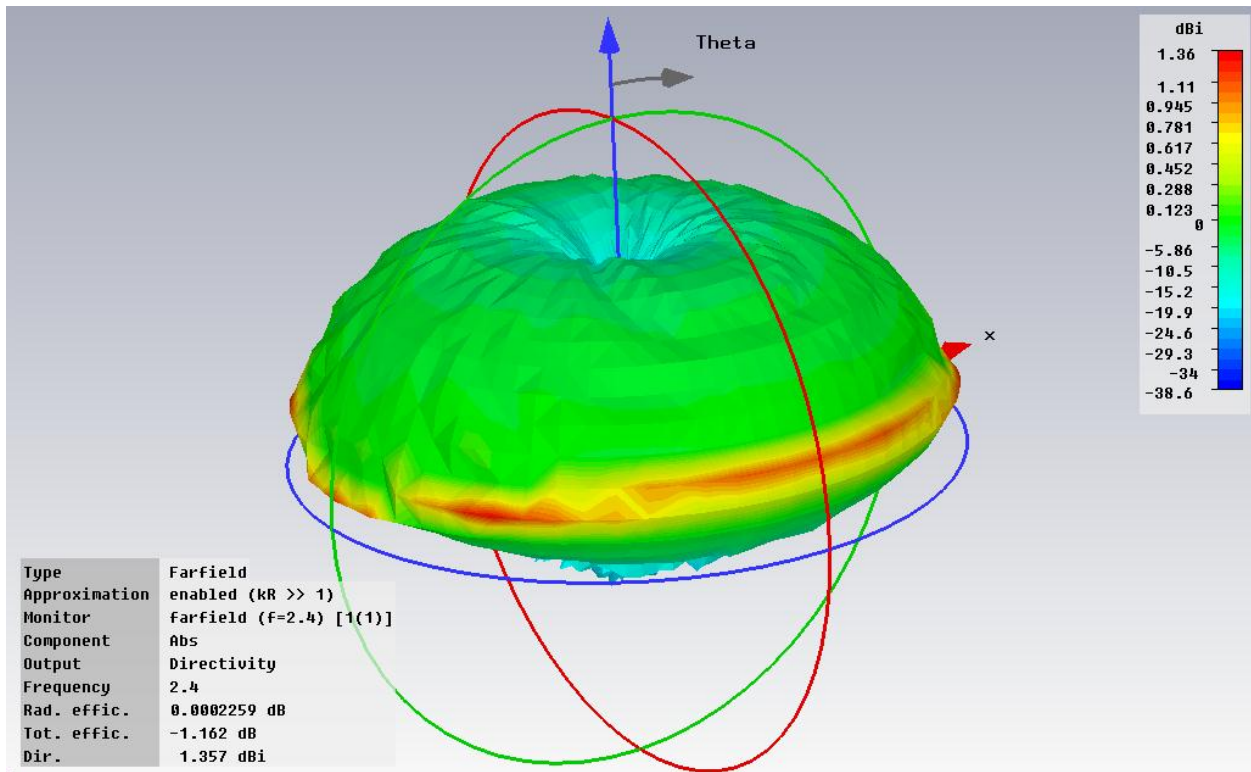


Figure 2.13 Scenario 1-Roof mounted antenna on boxcar: Farfield pattern

In the following figure we have illustrated the E-field strength at the surface of the 3d models (railcar and track). We can clearly see that the signal is at its strongest on top of the

boxcar roof closest to the antenna. The farther we get away from the antenna, the weaker the signal becomes. Furthermore, there is a significant decrease when we transition from the top of the boxcar to the side of the boxcar even though the distance increase of that transition is negligible. This is a result of the roof structure acting as an RF shield. It prevents most of the signals from propagating into the lower hemisphere—the area below the monopole including the entire boxcar area. As a result, field strength sharply diminishes at the sides of the boxcar.

However, as a result of the EM-field interacting with the object through signal diffraction, EM coupling, and so forth, we do observe some signals below the monopole antenna’s horizon, even in areas directly below the boxcar itself.

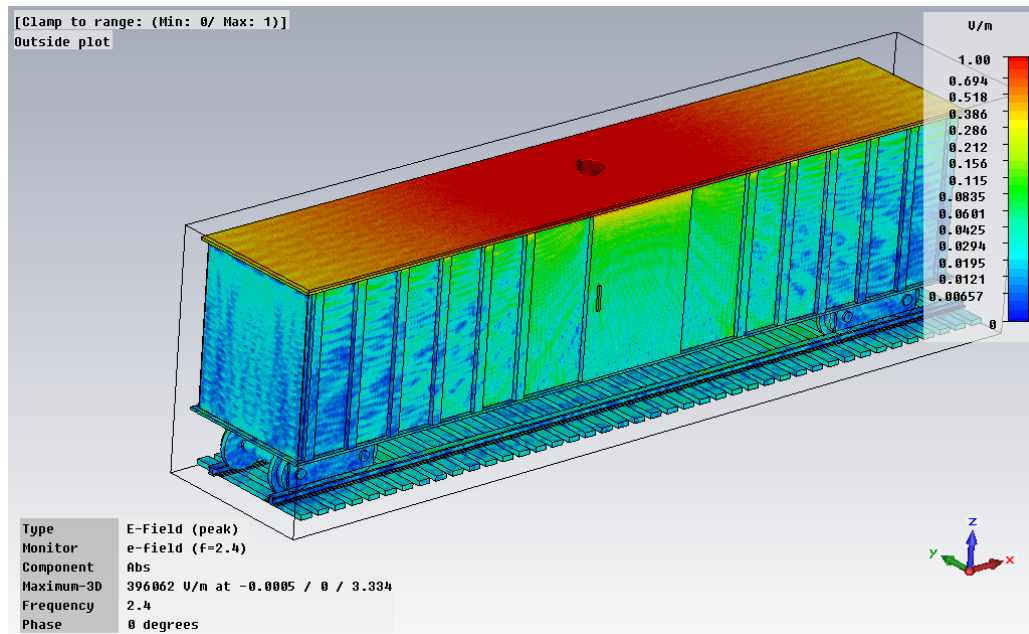


Figure 2.14 Scenario 1-Roof mounted antenna on boxcar: E-Field Visualization

2.4.2 The side-mounted antenna simulation

In this section we study a different placement of the monopole antenna. We relocated it to the side of the boxcar and mounted in the middle of the sliding door. We also reoriented the

antenna, now oriented horizontally in its new position, pointing away from the sliding door instead of upwards.

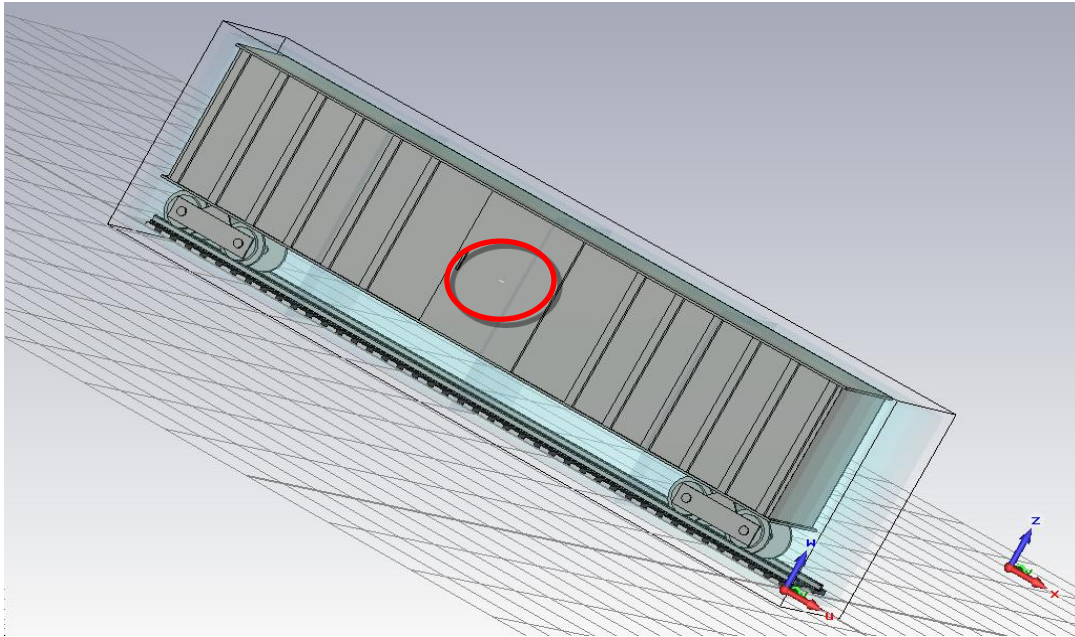


Figure 2.15 Scenario 2-Side mounted antenna on boxcar: Placement

We also reevaluated the resulting antenna pattern and found significant disturbances in the farfield pattern, as shown in the following figure. These distortions are the result of the vertical support struts that create signal impairments unlike the smooth roof structure, and are easily observed in the E-field illustration. In this illustration we can also see a particular effect that is the result of the model's door handle. It results in two significant horizontal E-field strength improvements, both at the top and bottom edge of the handle. We can also observe that the E-field is significantly more distorted with local disturbances throughout the entire field as compared to the case of the roof-mounted antenna. These disturbances are the result of the E-field interactions with the complex metallic structure at the side of the boxcar.

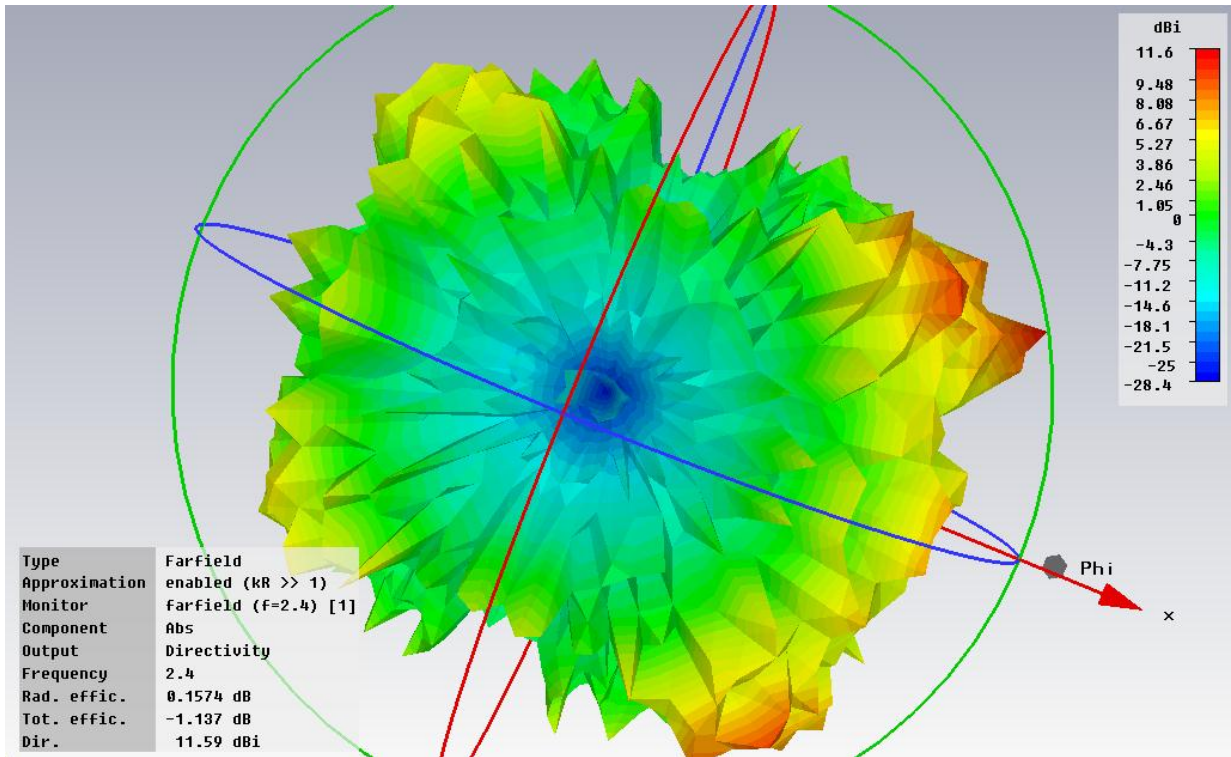


Figure 2.16 Scenario 2-Side mounted antenna on boxcar: Farfield Pattern

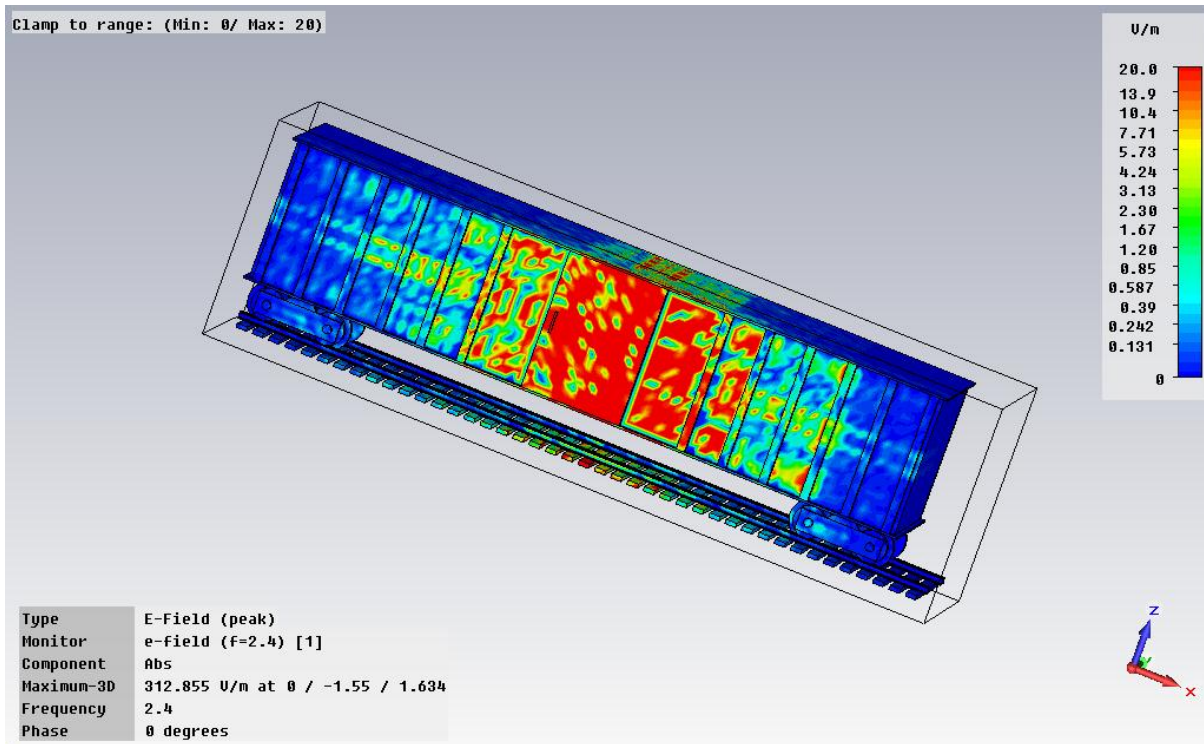


Figure 2.17 Scenario 2-Side mounted antenna on boxcar: E-Field Visualization

In the third simulated scenario we have repositioned the antenna once more. It is located at the undercarriage structure, close to the front wheel and brake assembly. This location was evaluated as a potentially vital location for wheel imbalance and brake status sensors, as is shown in the following figure. The antenna orientation has been adjusted back to a vertical orientation similar to the roof-mounted antenna.

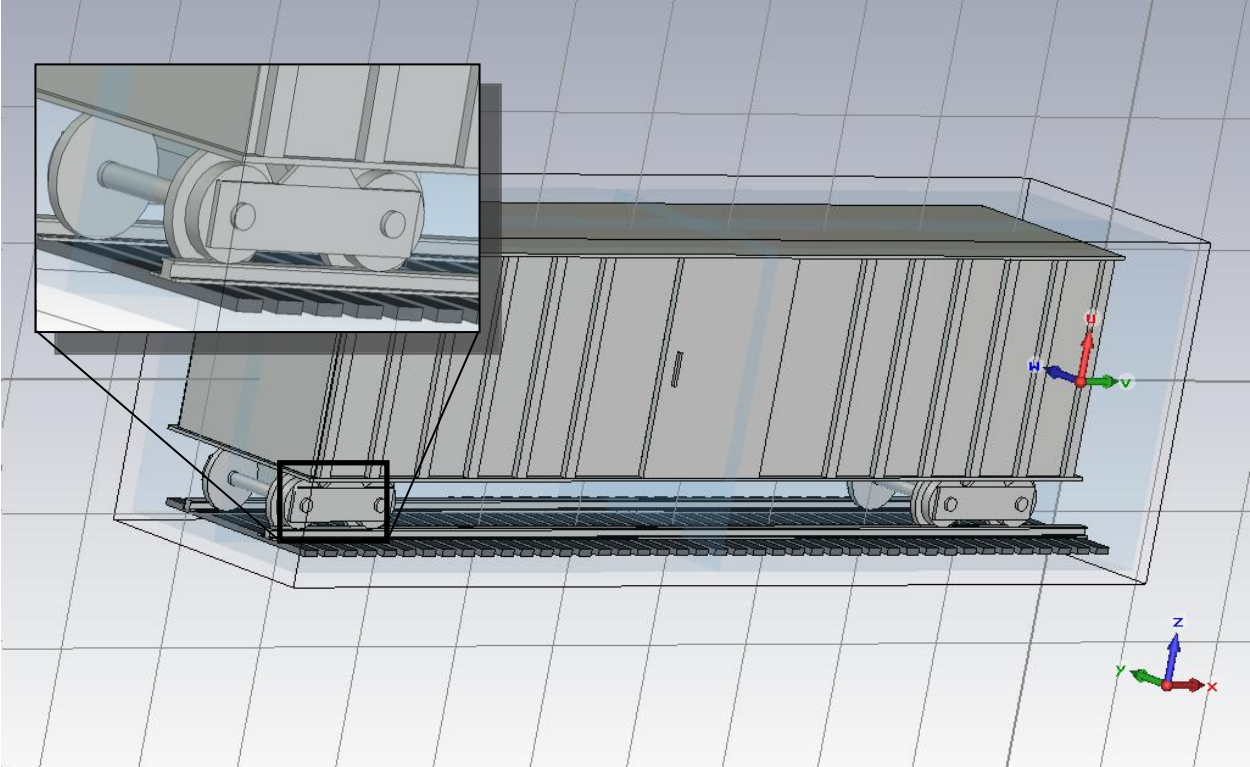


Figure 2.18 Scenario 3-Undercarriage mounted antenna on boxcar: Placement

In accordance with the previous two scenarios we simulated once more the antenna's farfield radiation pattern once more, shown in the following figure. Clearly, the amount of distortions to the monopole's antenna pattern has increased dramatically. The original donut shape has become all but unrecognizable.

In addition, the E-field visualization clearly shows the severe signal propagation limitation incurred around this transmitter location. The signal is limited to the area close to the transmitter only, and becomes too weak for reception at less than half the length of the boxcar—this is the result of the steel structure of the boxcar above the undercarriage. It deflects most of the signal’s energy downwards and thus prevents proper signal propagation along the railcar’s box structure.

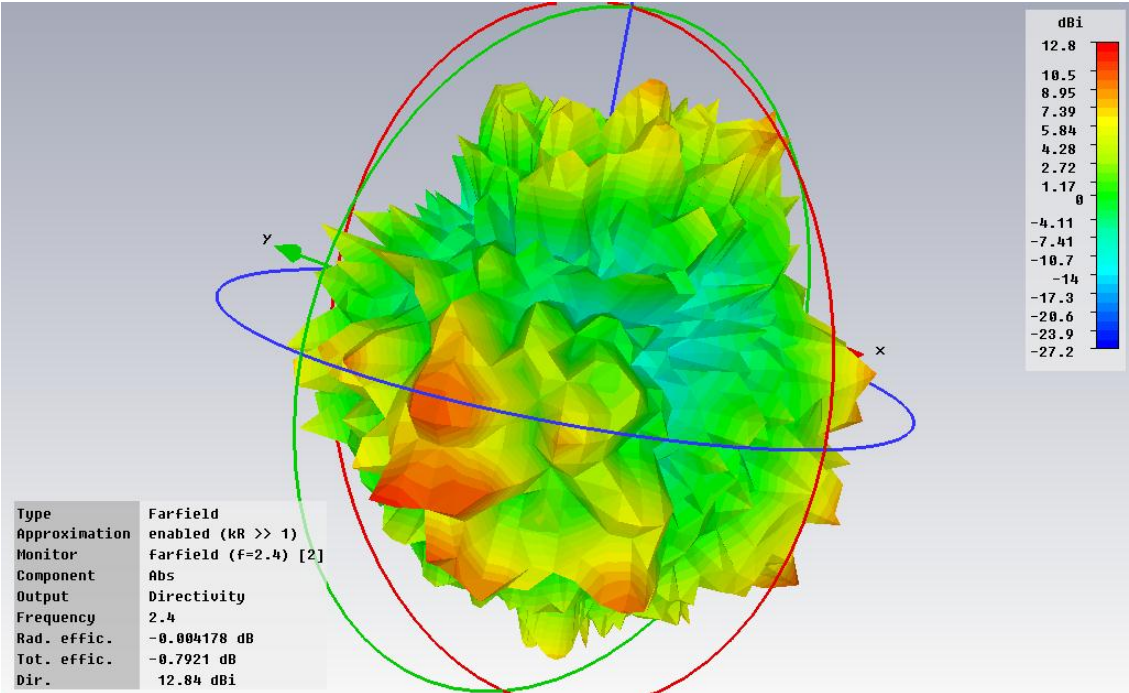


Figure 2.19 Scenario 3-Undercarriage mounted antenna on boxcar: Farfield Pattern

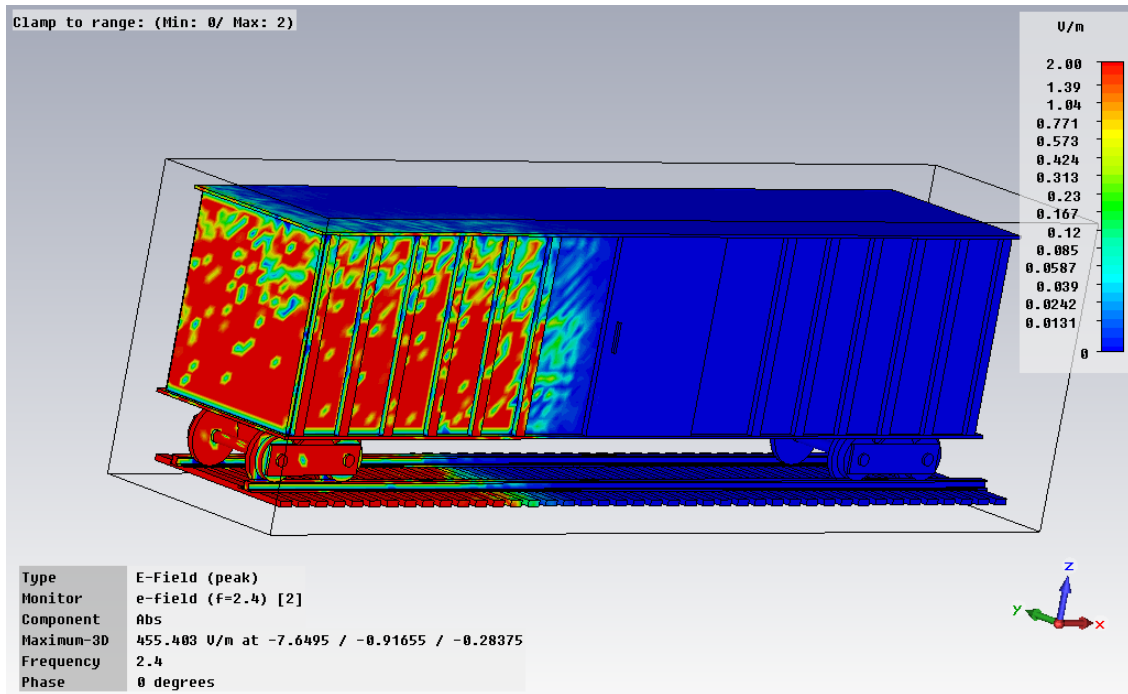


Figure 2.20 Scenario 3-Undercarriage mounted antenna on boxcar: E-Field Visualization

To better visualize this rapid loss in signal strength we have used the simulation results, by the software labeled as power flow, to plot a received signal strength decrease alongside the long axis of the boxcar. The small inset in the following figure shows the path along which this analysis is performed, displayed as a red line. The start location is on the left side and is associated with distance 0, progressing from this point towards the right side. The resulting RSSI reduction clearly shows a rapid drop in power flow at a distance around 5-6 meters from the start of the boxcar, with a total boxcar length of 15.8 meters as shown before.

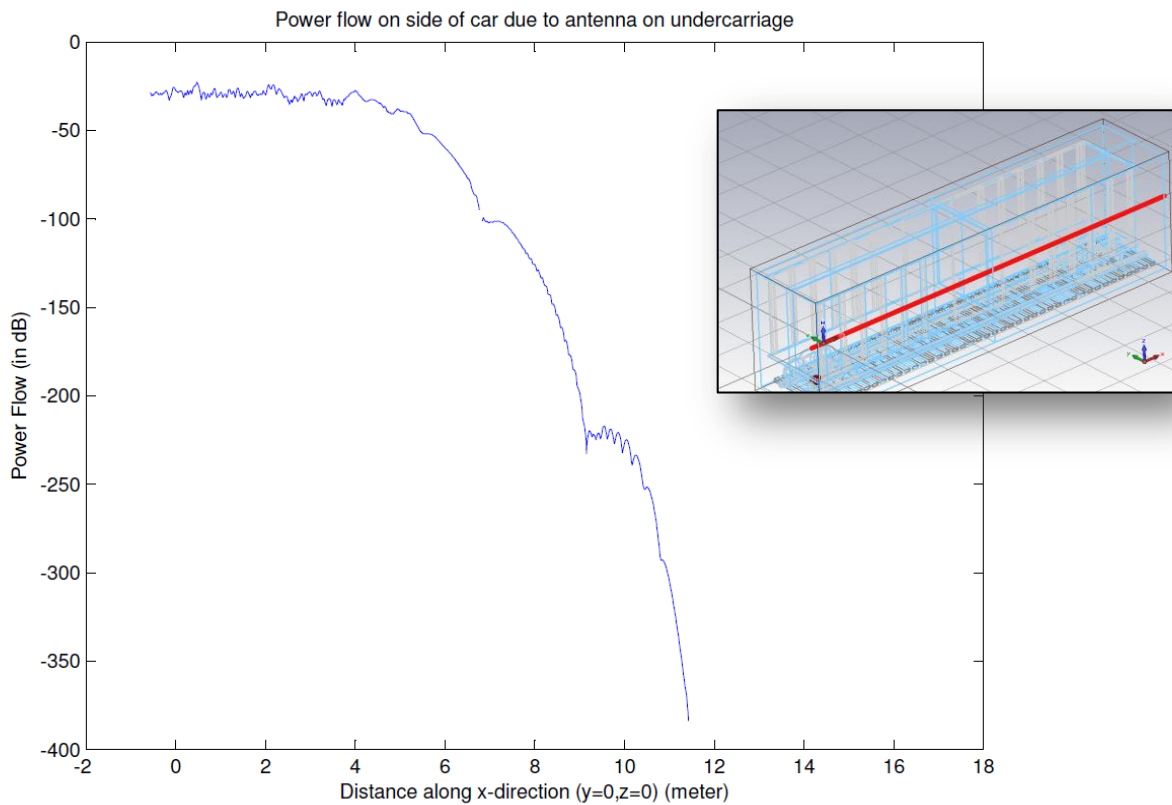


Figure 2.21 Scenario 3-Undercarriage mounted antenna on boxcar: Power Flow Analysis

In the fourth scenario we simulated the interaction between two passing railcars, one of which is equipped with a roof-mounted transmitter, and analyzed the resulting signal and field strength around both railcars. The following figures show the transmitter location and farfield pattern.

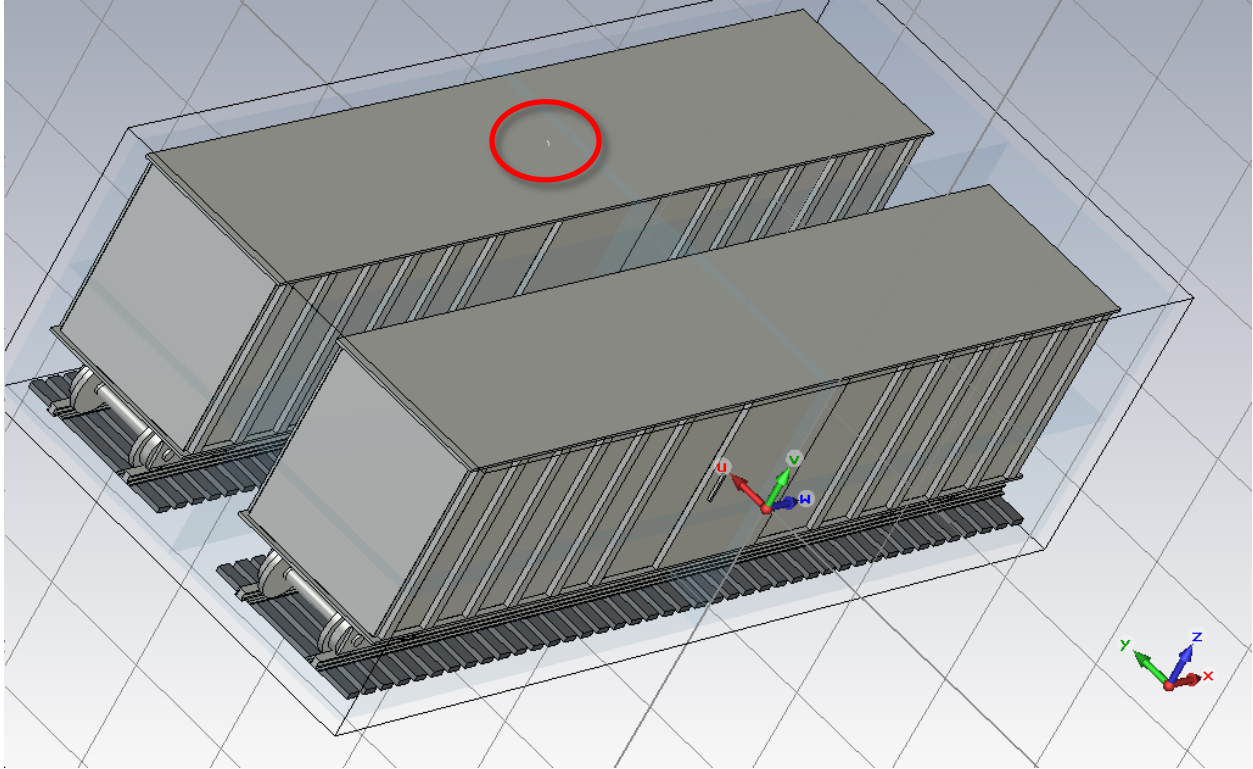


Figure 2.22 Scenario 4-Roof mounted antenna on boxcar passing train: Placement

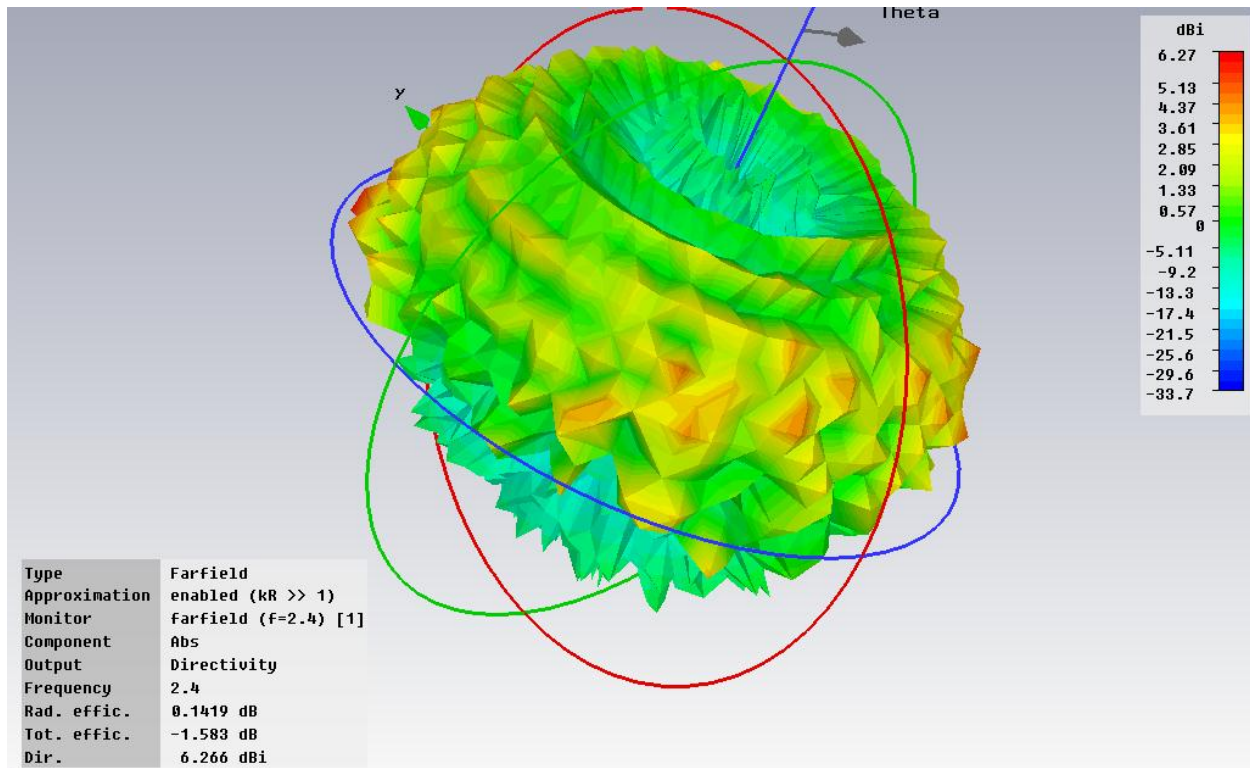


Figure 2.23 Scenario 4-Roof mounted antenna on boxcar passing train: Farfield Pattern

The farfield pattern shows some distortions, but far less than we observed during the undercarriage-mounted antenna test. In the following figure we are showing the E-field strength visualization. Clearly, the signal distribution is strongest over the roofs of the two railcars. We can also observe that the signal strength at the side of the railcar between the two railcars is stronger than the field strength observed in the case of a single railcar with roof-mounted antenna. This is a result of the signal “bouncing” between the two sides, interacting with the materials in the process. The outside vertical surface along the long axis indicates a drastic loss in field strength, attributed to the increase in distance and the additional signal obstruction between the transmitter and this surface.

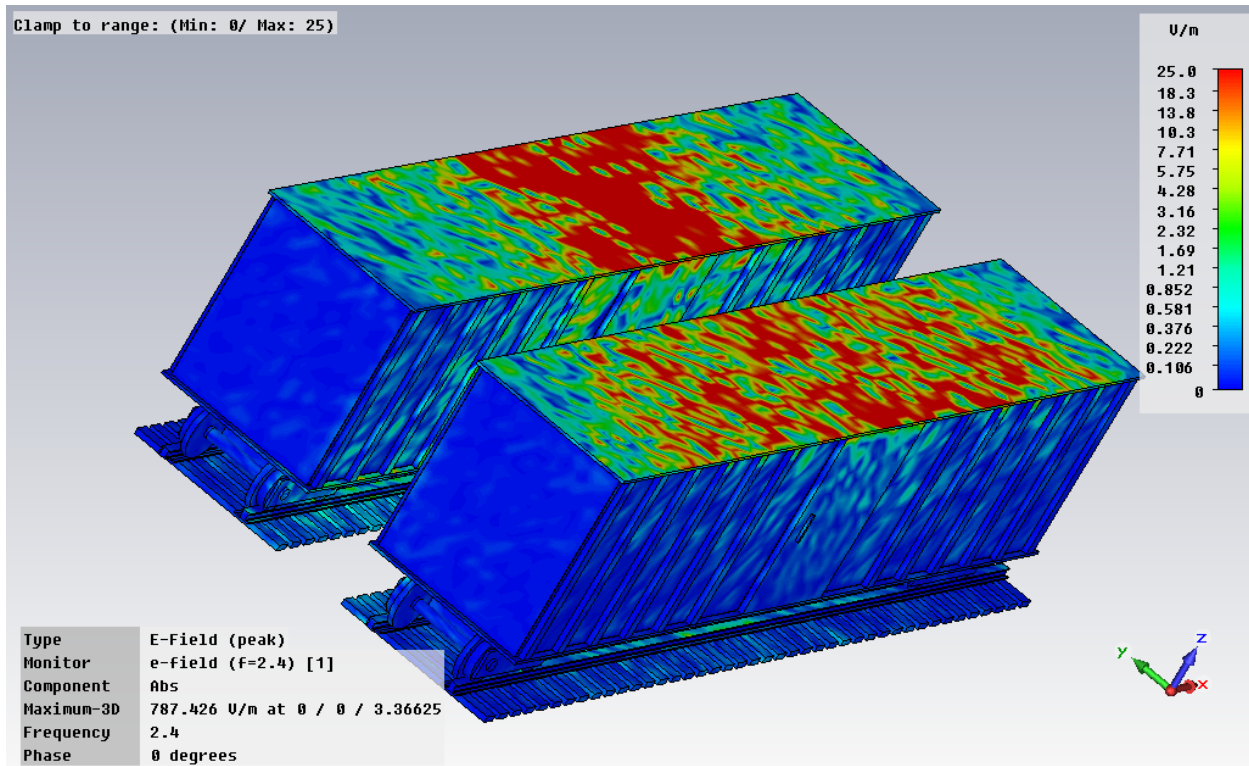


Figure 2.24 Scenario 4-Roof mounted antenna on boxcar passing train: E-Field Visualization

In the final scenario we evaluated, the dual-railcar topology was changed to a serial, back-to-back arrangement instead of a parallel arrangement. This simulates a single train's segment with two railcars, rather than two passing trains. The antenna is roof-mounted on the left railcar for this scenario.

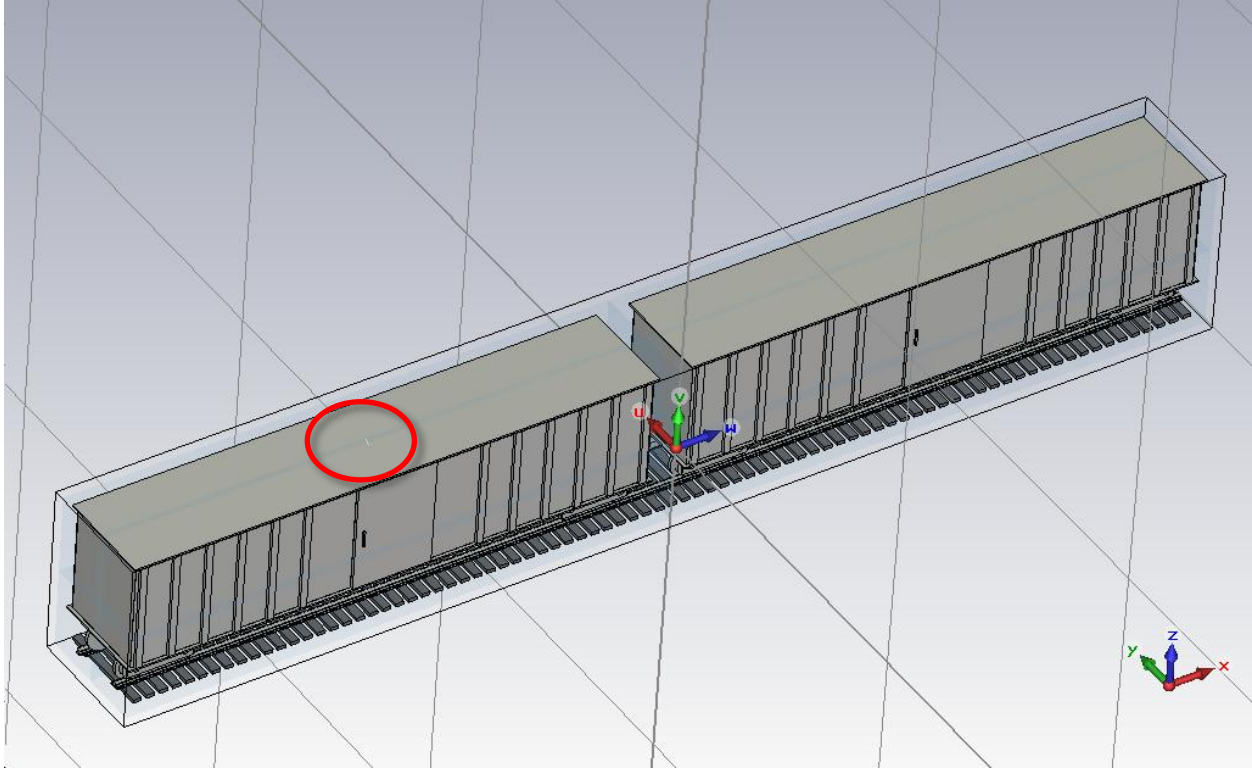


Figure 2.25 Scenario 5-Roof mounted antenna on boxcar in train segment: Placement

The observed farfield antenna pattern, shown in the following figure, is quite similar when compared to the farfield pattern of the scenario involving two parallel railcars. This conforms to our expectations as antenna placement and structure, as well as materials and signal obstacles, remain the same. Only the placement of one of the obstacles, the second railcar, has changed. However, since the first railcar's roof structure already blocks most of the energy from the southern hemisphere, the resulting farfield pattern remains largely the same.

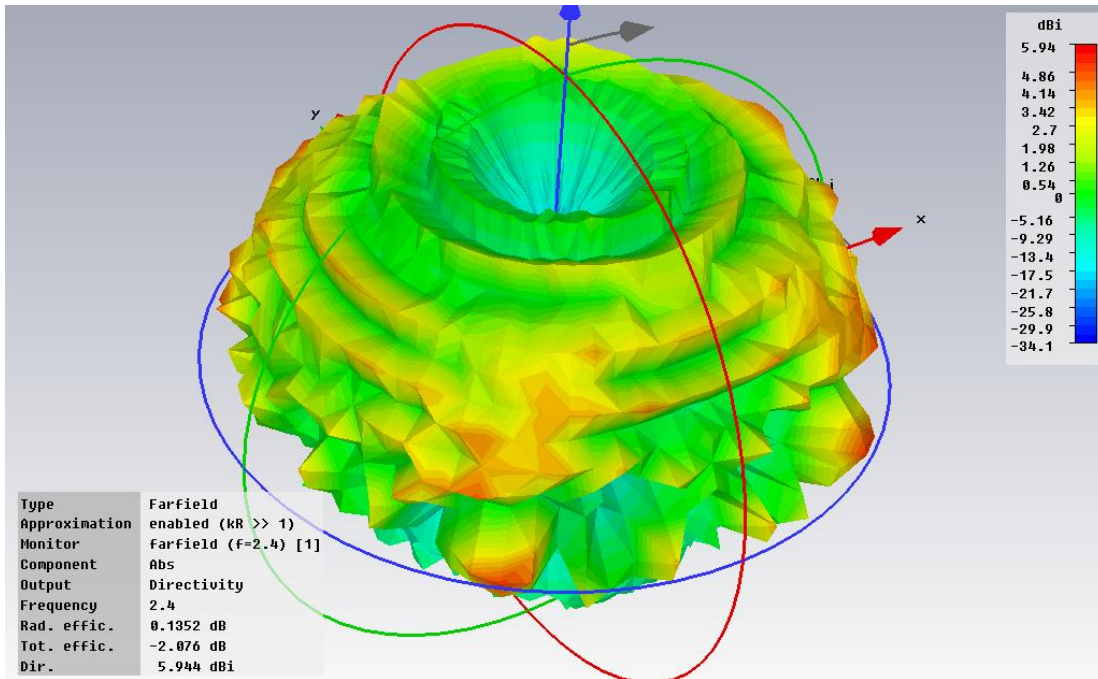


Figure 2.26 Scenario 5-Roof mounted antenna on boxcar in train segment: Farfield Pattern

In the following figure we visualize the E-field's strength in our final scenario. We can observe that the field strength provides a signal reaching from the middle of the left car's roof to a short distance onto the right railcar's roof. Field strength is also observed alongside the side of the first car, although no significant field strength is observed on the second car on the right-hand side of the simulated train segment.

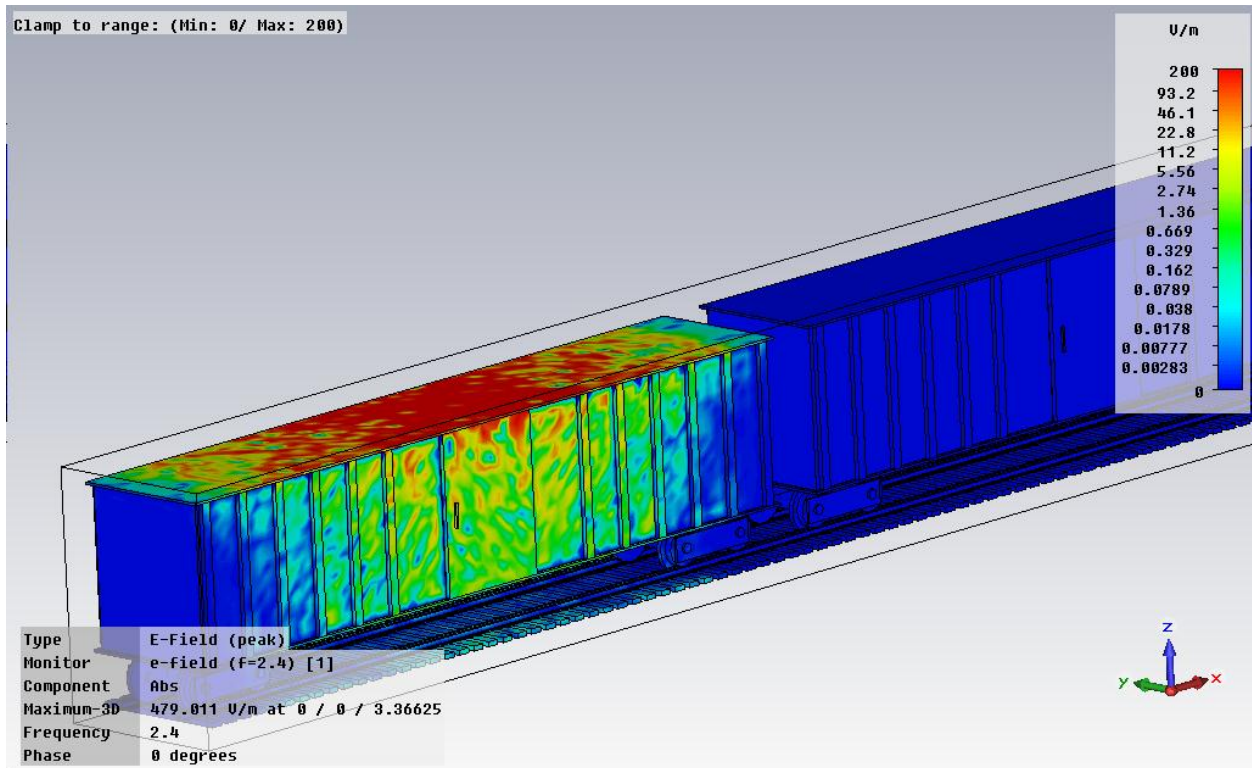


Figure 2.27 Scenario 5-Roof mounted antenna on boxcar in train segment: E-Field Visualization

Our simulations shown in this section indicate clearly that antenna placement is of significant importance in enabling desired communication distances. For our presented simulations, possible communication distances are typically limited to less than half the length of the boxcar, although high-sensitivity receivers would allow slightly larger distances. Placement of antennas on top of the roof of a railcar appears to provide the best signal propagation characteristics as expressed by the resulting farfield patterns. Placement at close proximity to the wheels appears to be the worst, requiring more transmitters onboard each railcar to relay the information over larger distances than is possible by the wheel-located transmitter itself. Finally, the structure of the railcar itself is also of importance, as shown by the E-field distortions in the various simulated scenarios.

To better understand these criteria we have simulated similar cases for each of our four railcar types. More of the obtained results are shown in the appendix.

2.5 Conclusions and Impact on wireless sensor networks onboard freight trains

Based on our findings from the propagation characteristics simulations we conducted using EM-Field Analysis we can derive the following conclusions.

- Placement of sensors is vital to the network design and depends on materials and structure in the design of the railcars.
- A single sensor is unlikely to have the communication range to span the distance equivalent of a single railcar.
- The closer the sensors are placed to the ground the more problematic its wireless communication will be.

Given these findings we now realize that simple placement optimization is not sufficient for creating freight train wireless sensor networks. We also need to consider the other protocol layers, in particular, the medium access control (MAC) layer and the routing layer. Given that with the limited communication distance we seem to require multiple wireless sensor nodes per freight railcar, routing becomes a critically important issue. With this many nodes sharing the same space, medium access control is also vital.

As a result, we decided to include a second research effort in our study of freight train wireless sensor networks, focusing on the protocol capabilities of the most commonly used wireless sensor network protocol, ZigBee. Our findings are presented in the following sections.

Chapter 3 Research Phase 2: Wireless Sensor Networks Protocol Study to evaluate performance capabilities

3.1 Methodology for WSN protocol study

Based on our expertise in evaluating network technologies and protocols for the Federal Railroad Administration over the past 5 years, we have opted for an approach that consists of two parallel efforts:

- a) The development of a comprehensive simulation model for studying WSNs in freight train environments and the development and evaluation of potential solutions to overcome problems discovered with current WSN technologies in this environment. For this part of the project we will utilize our expertise in developing physically accurate RF propagation simulation models.
- b) The implementation of existing or developed protocols on actual WSN hardware for use in field tests on rail cars and trains was provided by Union Pacific for this project.

By following this path we are able to collect valuable information that helps refine this technology in order to provide a robust and reliable platform that fulfills all the requirements the North American freight railroad industry has for this technology. The simulation models allow us to study a wide variety of scenarios without having to acquire and deploy costly equipment.

Based on the information collected from our discussion with Union Pacific we first wanted to verify the problems they encountered in their tests. To do so, we have tested standard wireless sensor network protocols on three well-known simulators: QualNet [8], OPNET [9], and NS-2 [10]. Although each of them comes with a basic sensor model, they have implemented it in slightly different ways. This initial study therefore also served as a comparison study between the different simulators to help select the most appropriate platform for our tests.

3.2 Evaluated Wireless Sensor Network Platforms

Throughout this entire study we received significant support from Union Pacific. In particular, their engineering expertise for railcar monitoring, and the wireless sensor network platforms they provided for our lab tests were invaluable to this project's success.

To validate some of our findings we used the two platforms shown in figure 3.1 in our lab tests.

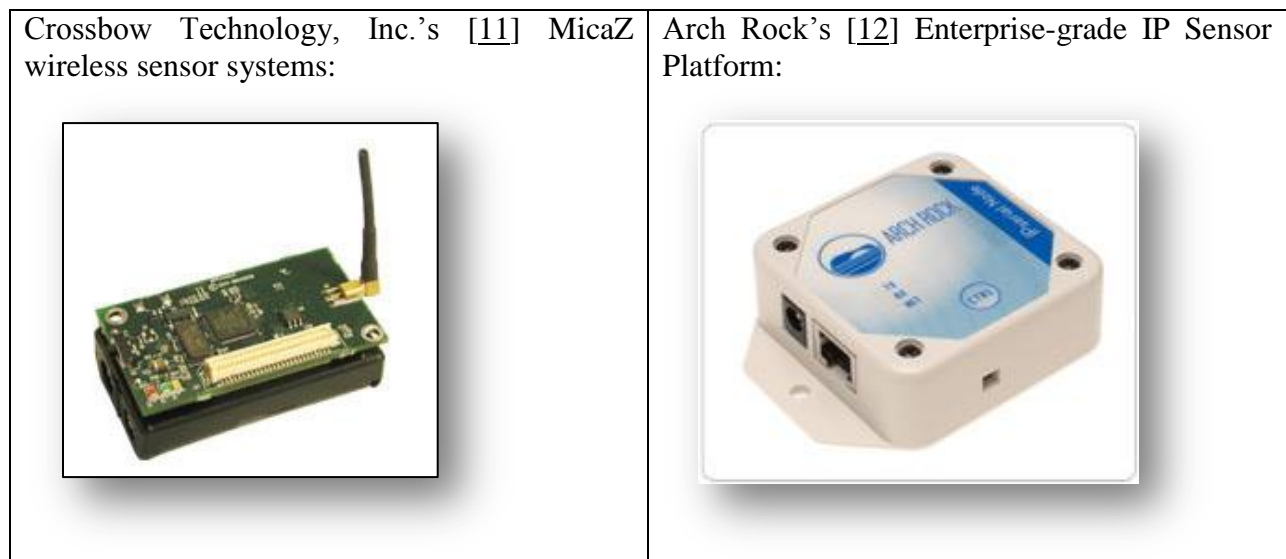


Figure 3.1 Evaluated Sensor Platforms

In our evaluation we could find that both systems' wireless links performed similarly under the same simulated link conditions. To test these systems we utilized our lab's Wireless Channel Emulator: the ACE-400WB [13] from Azimuth Systems. This system allows us to recreate virtually any wireless channel under controlled lab conditions. It allows for repeatable experiments, generating the same link every time we configure it. This is an invaluable tool in our lab performance evaluations.

3.3 Qualnet Simulator

QualNet's sensor network library is based on the IEEE 802.15.4 standard, also known as ZigBee. ZigBee is a Personal Area Network (PAN) technology, originally developed for communication between devices in very close proximity to a person, similar to Bluetooth. Hence, ZigBee provides a smaller per-node coverage area than technologies such as Wi-Fi and WiMAX, but it is more suitable for low-power devices such as Wireless Sensor Nodes.

ZigBee in QualNet provides implementations for the PHY and MAC protocol layers. Three modulation schemes have been implemented in the current model:

- a) O-QPSK with DSSS in 2.4 GHz frequency band,
- b) BPSK with DSSS in 868/915 MHz frequency band, and
- c) PSSS with BPSK and ASK in 868/915 MHz frequency band.

The two most critical elements are the PAN coordinator and PAN router. A PAN coordinator basically starts the network. It is the original discoverable device and provides a network name and methods for synchronization between nodes of the same network. PAN routers are devices that join an already existing network advertised by a PAN coordinator and provide data forwarding functionality through the network.

The MAC protocol supports two operation modes: beacon-enabled mode and non-beacon-enabled mode. In a typical ZigBee network there are different roles for network nodes. The MAC protocol implementation utilizes non-slotted CSMA/CA in non-beacon-enabled mode, whilst in beacon-enabled mode it is the PAN coordinator's responsibility to periodically generate beacons to synchronize nodes that are associated with it. In beacon-mode, all nodes belonging to the PAN coordinator are required to be in sync since it uses a time-slotted approach for

communication. Other features that have been included in QualNet are energy detection (ED), a battery model, an RF energy consumption model, and Link Quality Indication (LQI).

The initial network configuration for our tests simulates a scenario with a single long train by setting up a simulation of about 50 hops. We assume that each rail car contains one ZigBee router in order to forward packets between its adjacent neighbors. ZigBee router nodes also forward beacon messages so that nearby ZigBee devices can associate with the network. The PAN coordinator is located at the locomotive at the front of the train. Two ZigBee end devices were also created. These are virtual devices that simulate applications, or the data source and sink. The data sink end point is located at the PAN coordinator in the locomotive (the left-most node) while the data source node is located in the last freight car (the right-most node). The source generates small data packets at a rate of 1 packet every 10 seconds. Each data packet is then transmitted through the PAN network towards the data sink at the locomotive. Figure 3.2 is a screenshot of the topology setup in the QualNet network simulator environment. All sensors are in the same network. Each individual node's communication range is short. Thus, each node can communicate only to its neighboring nodes and depends on the ZigBee routing functionality to forward the data to the data sink.

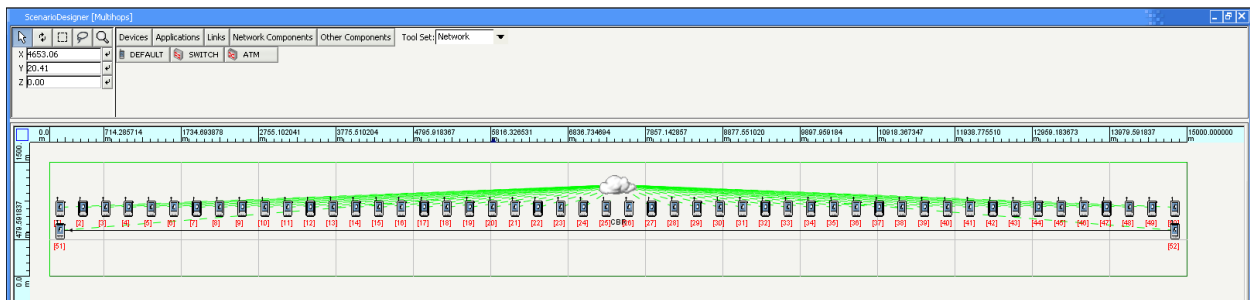


Figure 3.2 Simulation Setup in QualNet

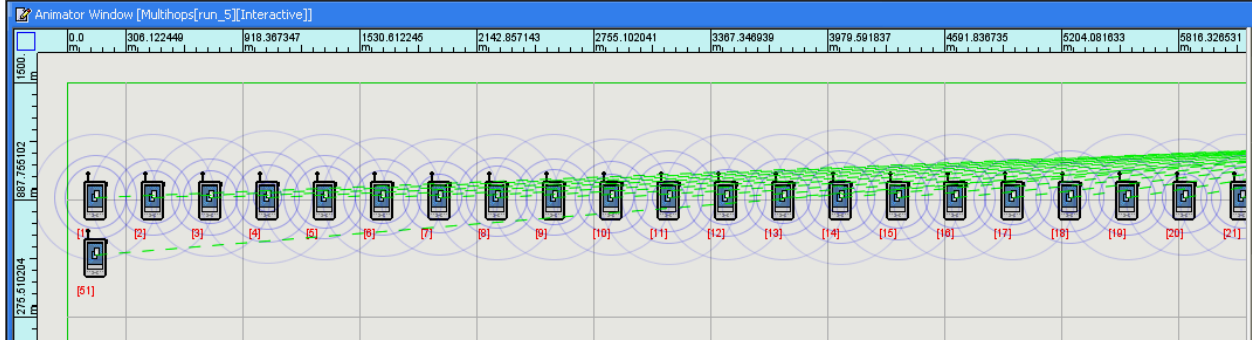


Figure 3.3 Beacon Synchronization

In beacon-enabled mode, beacon frames are periodically sent by the PAN coordinator to identify its PAN and synchronize nodes that are associated with it. Following each beacon is an active period (superframe) during which data communication occurs and an inactive period. The duration between two consecutive beacon frames is called the Beacon Interval (BI). The BI and the Superframe Duration (SD) are determined by two parameters: the Beacon Order (BO) and the Superframe Order (SO), respectively. The BI is defined as follows:

$$BI = aBaseSuperframeDuration \cdot 2^{BO}, \text{ for } 0 \leq BO \leq 14.$$

The SD is defined as:

$$SD = aBaseSuperframeDuration \cdot 2^{SO}, \text{ for } 0 \leq SO \leq BO \leq 14.$$

In both formulas $aBaseSuperframeDuration$ is the minimum duration of the superframe, corresponding to $SO=0$. At 2.4 GHz band, $aBaseSuperframeDuration$ is 15.36 milliseconds. In our simulation, we set both BO and SO to 4. This means that the beacon interval is 245.76 milliseconds (approximately 4 beacon frames per second). The overall simulation duration is configured to be 1,000 seconds. Thus, the PAN coordinator generates around 4,000 beacon frames during the entire simulation. After a ZigBee router within the PAN coordinator's communication range hears the beacon frame, it tries to associate to the PAN coordinator. This

process is called Network Discovery. After having successfully associated with the PAN, the ZigBee router starts forwarding beacon frames to enable its neighbors to join the network as well. This process is repeated by each subsequent hop until the last ZigBee router has synchronized to the PAN network. As can be seen in the left chart of Figure 3.4, the first node (PAN coordinator) transmits 4,066 beacon frames while the last node (data source in the last freight car) transmits 3,755 beacon frames. Given the difference in beacons transmitted and the beacon interval, this means that it took about 80 seconds to synchronize the entire network.

This provides a significant delay even before normal network operations can be started and constitutes a major problem for dynamic network operation. Imagine a rail yard where rail cars are constantly moved among trains. Each time this occurs the network topology of a train changes and thus all nodes need to be re-synchronized.

However, the main problem of this multi-hop simulation is not beacon synchronization, but routing. As our simulations show, route discovery provides an additional and even more significant delay. Even though the first data packet in our simulation has been generated at the ZigBee data source at the 10th second, the first packet arrived at the PAN coordinator's data sink at the 250th second. It took about 4 minutes just to establish a data path through 50 hops! Additionally, this process may also have to be repeated at every network entry or exit of nodes, similar to re-synchronization. These findings correspond closely with the problems reported by Union Pacific for their tests.

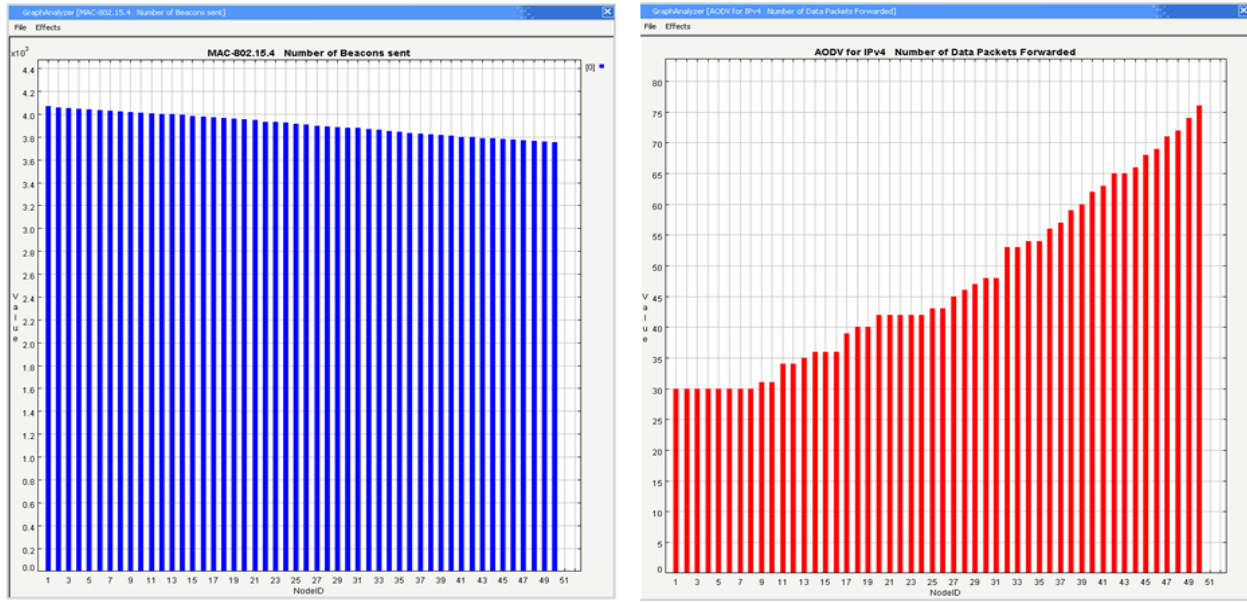


Figure 3.4 Average No. of Beacons sent (left) and Average No. of data packets forwarded (right) in our QualNet simulations

From the right-hand chart in Figure 3.4 we can identify another problem found in wireless communication systems: packet loss. We can see that, while we actually generated 98 data packets at the source node, only 76 data packets are received by the first neighbor and only 30 packets managed to reach the destination. In other words, less than a third of the data packets managed to reach the destination. This can be attributed to bit errors occurring at each receiver and, since ZigBee does not provide a mechanism for retransmission of erroneous packets, the discarding of all these failed transmissions. While each individual link may even exhibit a fairly low packet loss rate, this problem is compounded by the large number of hops. This is the Achilles heel in networks that use this particular topology of long node chains.

3.4 OPNET Simulator

Although OPNET claims that it also provides a ZigBee model, only a few functions of the ZigBee protocol have been fully implemented so far. The PHY layer is very simple and

abstract: there is no modulation scheme. Packet reception is determined by a single threshold only. If the received signal power is lower than the threshold the packet is dropped, otherwise it is received successfully. No bit error rate calculation or channel model is implemented. The MAC protocol supports only a non-beacon-enabled mode which utilizes non-slotted CSMA/CA. Neither the slotted mode nor the contention-free operation mode is supported. Another limitation in OPNET is the maximum number of hops. At the moment, the model only supports star, tree, and mesh topologies. For the tree and mesh topologies, the maximum depth is 15 hops from the PAN coordinator. In other words, we can at best set up a 15-hop simulation scenario.

Nevertheless, to test this implementation we set up a 15-hop simulation in OPNET with non-beacon-enabled mode. Similar to the QualNet simulation we assume that each freight car contains one ZigBee router. In this simulation, however, node 17 is the data sink. The data source is node 1, which not shown in Figure 3.5 but is located at the left-most end of the chain topology. The data source generates small data packets at a rate of 1 packet each second.

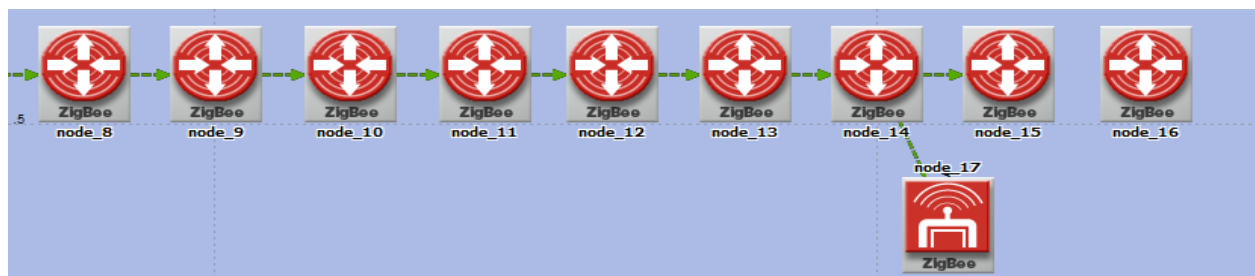


Figure 3.5 Simulation topology for OPNET

Figure 3.5 is the node layout in our OPNET simulation. All sensors belong to the same PAN network and, as can be seen in the figure, the green arrows show the direction of traffic flow from left to right. Node 14 broadcasts the data packets it received from node 13. These

forwarded messages are then received by both node 15 and node 17, however, because the packet destination is set to be node 17, node 15 will discard these packets. To test the hop limitation we then moved node 17 one node to the right such that it connects to the network through node 15 instead. As a result of this change, the hop count between data source and sink is now 16 and thus exceeds the OPNET model's limitation. Therefore, node 16 received no data packets at all. This is a severe limitation in the ZigBee implementation in OPNET, but it is not a limitation resulting from the ZigBee protocol itself.

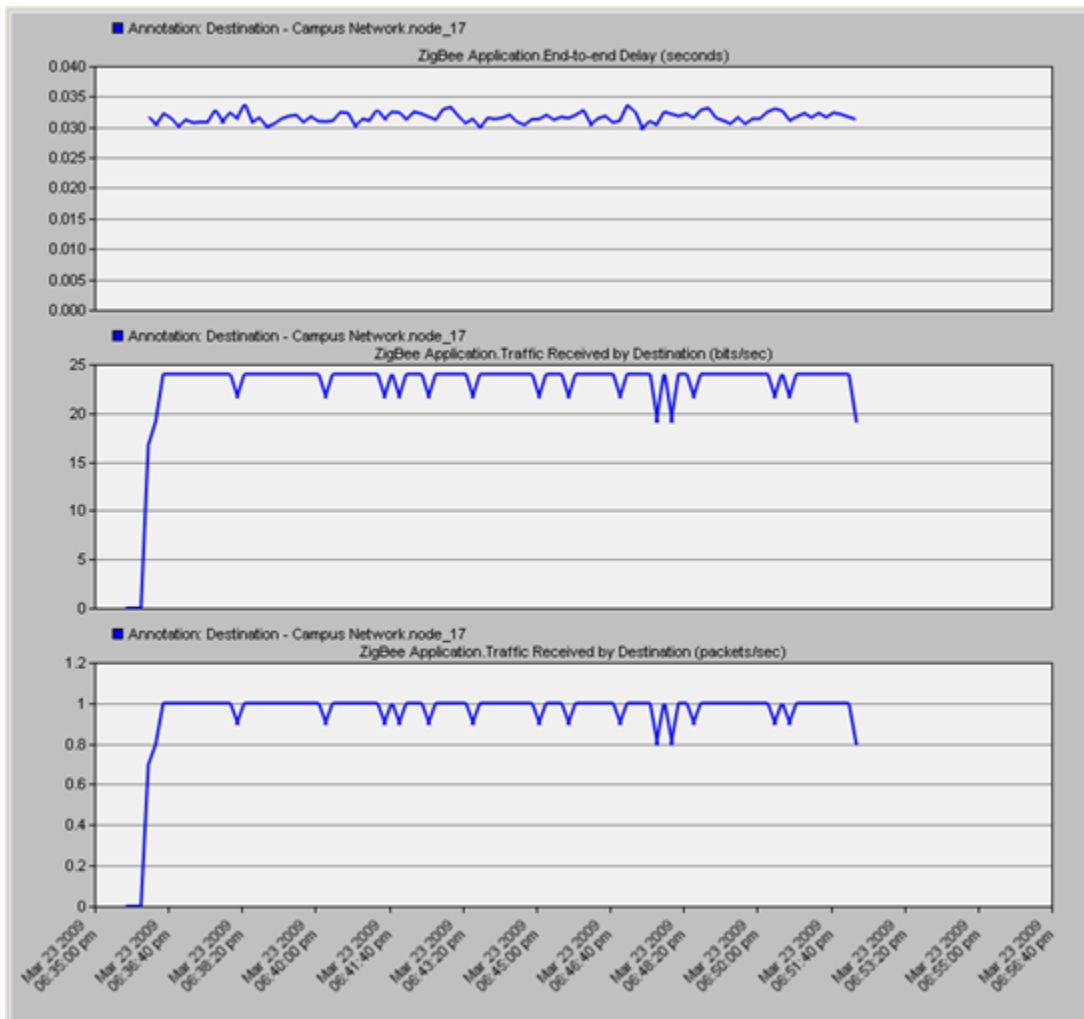


Figure 3.6 End-to-end delay and throughput results collected from OPNET simulator

We have collected end-to-end delay and throughput at the sink node (node 17). Figure 3.6 shows the results obtained from the OPNET simulator. The first graph shows the application layer end-to-end delay measured in seconds. We can see that delay time is quite low even for the first packet. This results from the lack of beacon synchronization delay since the OPNET model does not support the beacon-enabled mode. The time for route discovery is also very short, since we only have a network of 15 hops. As a result, route discovery was completed before the first data packet was generated. For the throughput in the second and the third graphs, the destination has received packets at approximately 1 packet per second or 24 bytes per second (OPNET mislabeled the graph as bits/sec instead of bytes/sec).

The occasional reductions in received throughput or packets are not the results of bit errors, since OPNET's ZigBee module does not calculate bit errors or frame errors at all, but rather a result of its statistics collection and processing system.

3.5 NS-2 Simulator

The third simulator with support for ZigBee simulation we tested is ns-2. Similar to OPNET, there is no support for bit error simulation at the moment. Packet reception is determined by a simple receive threshold. The MAC protocol in ns-2 supports the operation for both non-beacon-enabled mode and beacon-enabled mode. The ns-2 simulator supports pure CSMA-CA and slotted CSMA-CA with star and peer-to-peer topologies. Similar to QualNet, ns-2 features beacon tracking and synchronization. Other features which have been included in ns-2 are energy detection (ED), clear channel assessment (CCA), and link quality detection (LQD).

We set up a train scenario in ns-2 similar to our QualNet simulation using 50 rail cars. The PAN coordinator is located in the first freight car (node 0) and also acts as the data sink node (labeled as node 51). The data source is at node 52 at the opposite end of the train. The

source sends small data packets at a rate of 1 packet per second to the data sink at the PAN coordinator.

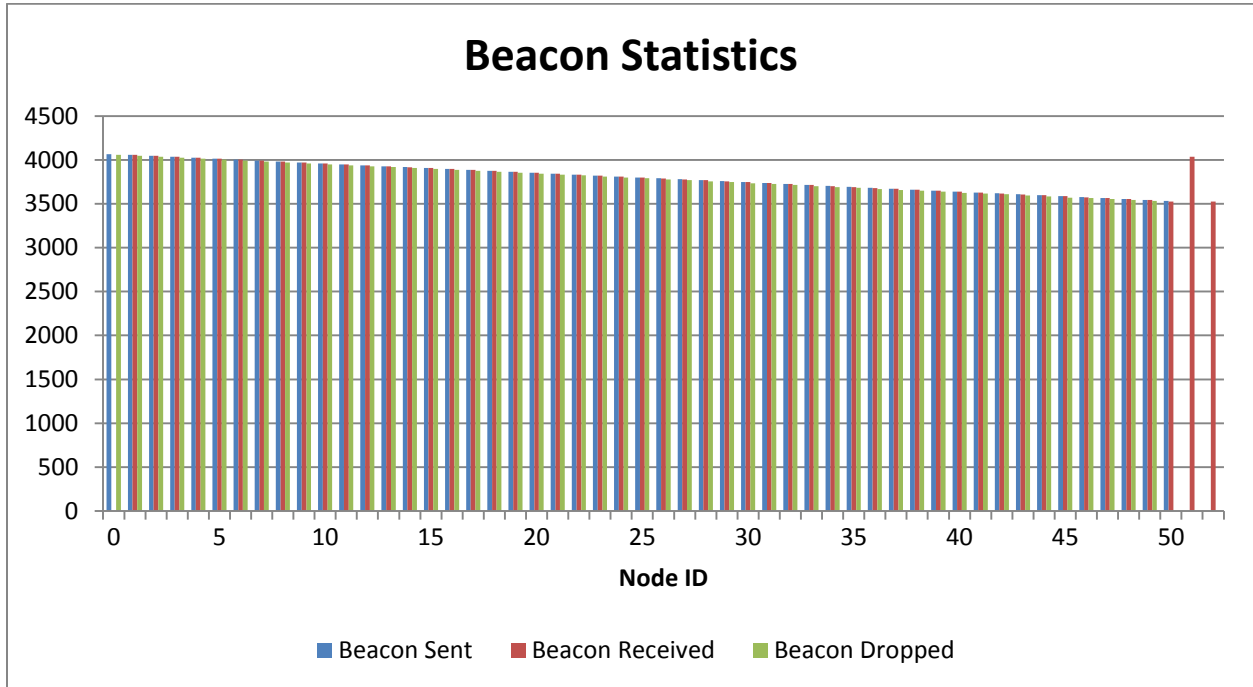


Figure 3.7 Number of beacon frames sent, received, and dropped in ns-2

The simulation duration is set to 1,000 seconds, similar to QualNet. Thus, we can expect that the PAN coordinator generates around 4,000 beacon frames for the duration of the simulation. As can be seen in Figure 3.7, the PAN coordinator transmits 4,066 beacon frames, while the data source node in the last freight car transmits only 3,533 beacon frames. Accordingly, the whole network takes about 131 seconds to synchronize all sensor nodes. Interestingly, this process takes about 50 seconds longer in ns-2 than in QualNet. We are currently investigating to obtain more insight into the source of this discrepancy.

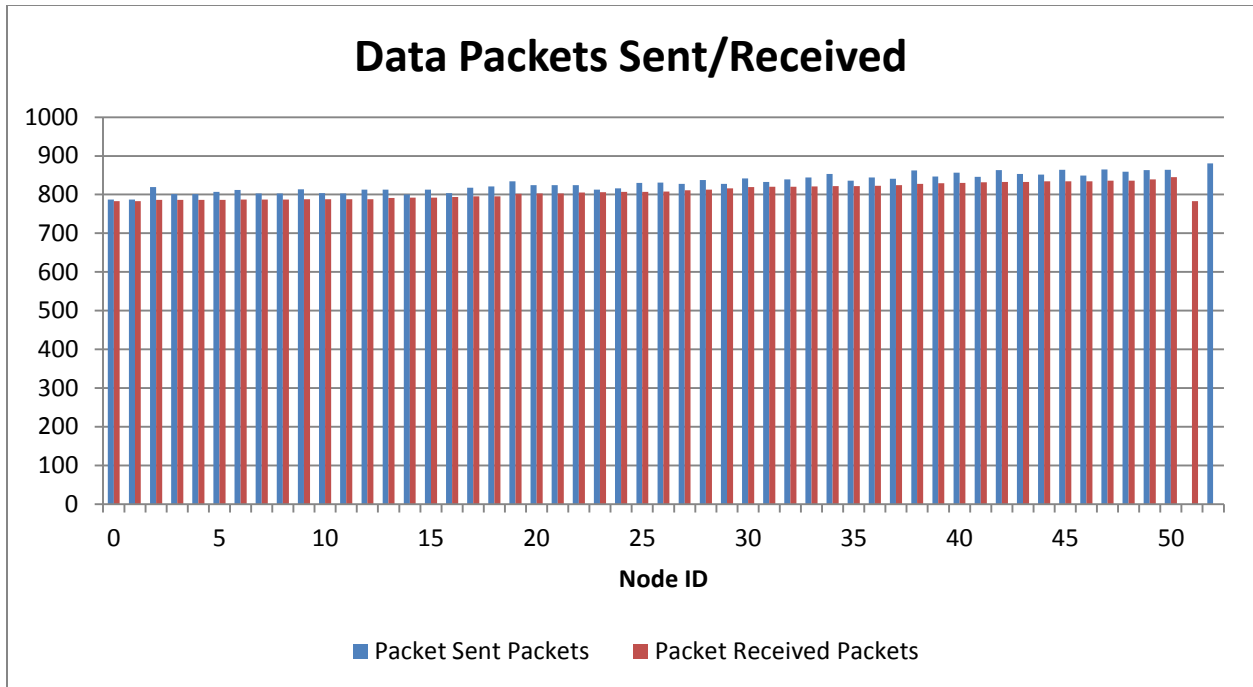


Figure 3.8 Number of data packets sent and received in ns-2

Figure 3.8 demonstrates the number of data packets sent and received for each node. We generated a total of 881 data packets at the source, out of which only 845 packets reached the first-hop neighbor and only 783 packets reached their destination at the data sink. Thus, the packet loss in this simulation is approximately 11%. This can currently only be attributed to simulation errors as there are no bit errors being simulated for this model in its current state.

In conclusion, none of the three evaluated simulators provide a complete wireless sensor network simulation model. All simulators exhibit problems, most of which can be attributed to either implementation problems or protocol issues. QualNet achieves network synchronization faster than ns-2 for the same configuration while ns-2 performs better in route discovery. Current limitations in OPNET all but eliminate it as a candidate for our simulation work. Our baseline simulations have helped us to identify the following critical issues and shortcomings in the standard ZigBee protocols for use in freight train WSNs.

- a) The large number of hops severely degrades network performance due to frequent synchronization and route update requirements. ZigBee is simply not designed for multi-hop networks with very large hop counts.
- b) The lack of per-hop retransmission schemes for erroneous packets creates several latency and robustness issues.
- c) The current ZigBee protocols do not cope well with topology changes.

Protocol changes are required to fix these issues. Our group's efforts in the past months have been directed at developing and testing potential solutions to these problems. These efforts are described in the following sections.

Chapter 4 Proposed Solution: Multi-layer Multi-hop Networks

4.1 Description

In order to solve the protocol problems we identified with our simulation study for large-scale multi-hop networks, we propose a multi-layer multi-hop network. The idea is to divide a long chain-topology network into multiple segments and connect those segments with a longer-distance communication system to reduce the number of hops required for route discovery and data forwarding. Figure 4.1 explains this approach.

Imagine a 100-car freight train. In order to deliver data from the end of the train to the locomotive and the PAN coordinator, we have to traverse 100 individual wireless hops. The probability for packet corruption and the subsequent discarding of the contained information approached 100% in such a scenario, resulting in an effectively crippled data network. Instead, our proposed approach would divide this network into groups of 10 cars each, resulting in 10 such groups. Each group has its own coordinator that also is equipped with a long-range wireless radio, such as Ad-Hoc Wi-Fi. Instead of 100 hops, now we need only to traverse 20 hops, drastically reducing the end-to-end packet loss rate, the end-to-end latency, the time required to synchronize the network as now each group synchronizes independently, as well as the routing issues resulting from the large number of hops in the original scheme.

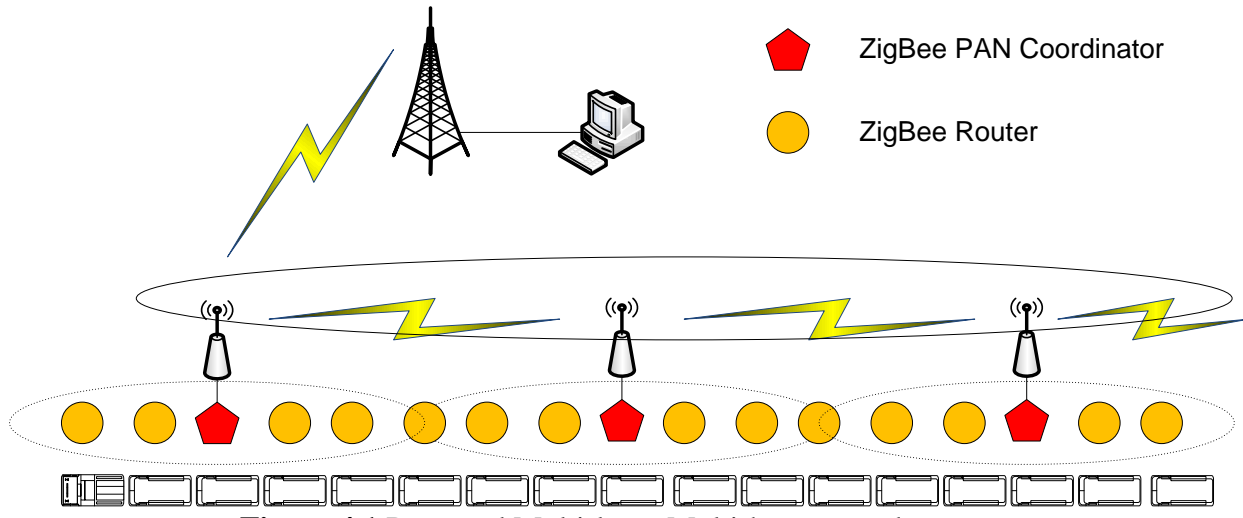


Figure 4.1 Proposed Multi-layer Multi-hop network strategy

For a higher-tier network technology we are currently studying Wi-Fi links to interconnect the WSN PAN groups, which provide longer range, more bandwidth, and faster data transfer rate. Our work for the Federal Railroad Administration has shown that Wi-Fi links have the capability to work over a distance of close to a mile, or 1600m, in a mobile railroad environment. Since the Wi-Fi communication range is relatively long, we can effectively skip over the individual WPAN hops and instead directly communicate between individual Wi-Fi radios attached to each PAN. This approach exhibits great promise to solve the problems associated with ZigBee multi-hop communication.

The advantages of this approach are:

- a) A dramatic reduction in total hop count,
- b) More bandwidth and faster data transfers using Wi-Fi as the top-tier technology,
- c) More flexibility, and
- d) Much higher reliability.

The costs of this approach are:

- a) Wi-Fi devices need to be attached to some or all PAN elements, and
- b) Higher power consumption for Wi-Fi-enabled PAN nodes.

4.2 Network Simulations

4.2.1 General Simulation Scenario

Let's assume the same scenario as in our previous simulations in which we have a train with 50 rail cars. If each car has one ZigBee router, we can now split this network into 10 individual PANs, each having 5 PAN nodes. Each PAN then has 1 PAN coordinator and 4 traditional ZigBee routers. Each PAN coordinator is also equipped with a Wi-Fi radio chipset for the higher-tier network. In this scenario, the maximum number of hops in WPANs can be decreased from 50 to 5, while 10 hops on Wi-Fi does not pose any problems for data flow as demonstrated in our tests for the Federal Railroad Administration.

4.2.2 QualNet

We first adapted our simulation in QualNet to incorporate this modified multi-tiered strategy for freight railroad WSNs. As can be seen in Figure 4.2, there are only 5 sensors in each WPAN. Wi-Fi devices connect together in Ad-Hoc fashion to form the top tier. At the locomotive we have also create a data sink. Instead of only having a single data source, for this simulation we have configured each sensor in the last WPAN to generate CBR traffic at 1 packet per second and the simulation duration is reduced to 100 seconds.

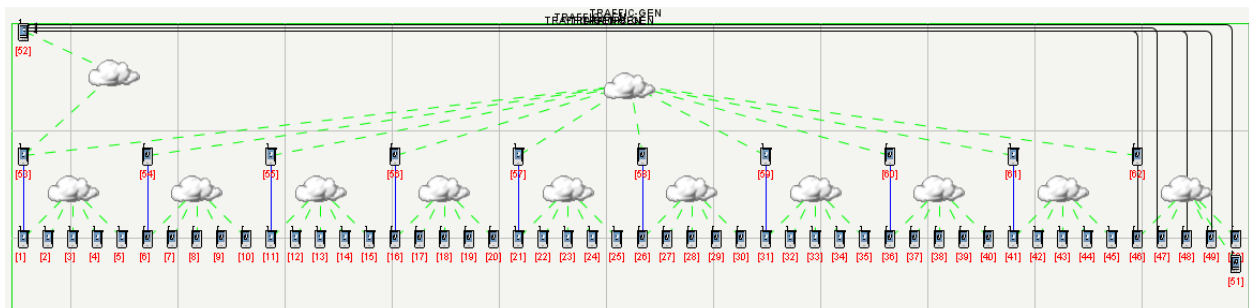


Figure 4.2 Multi-layer multi-hop wireless sensor network in QualNet

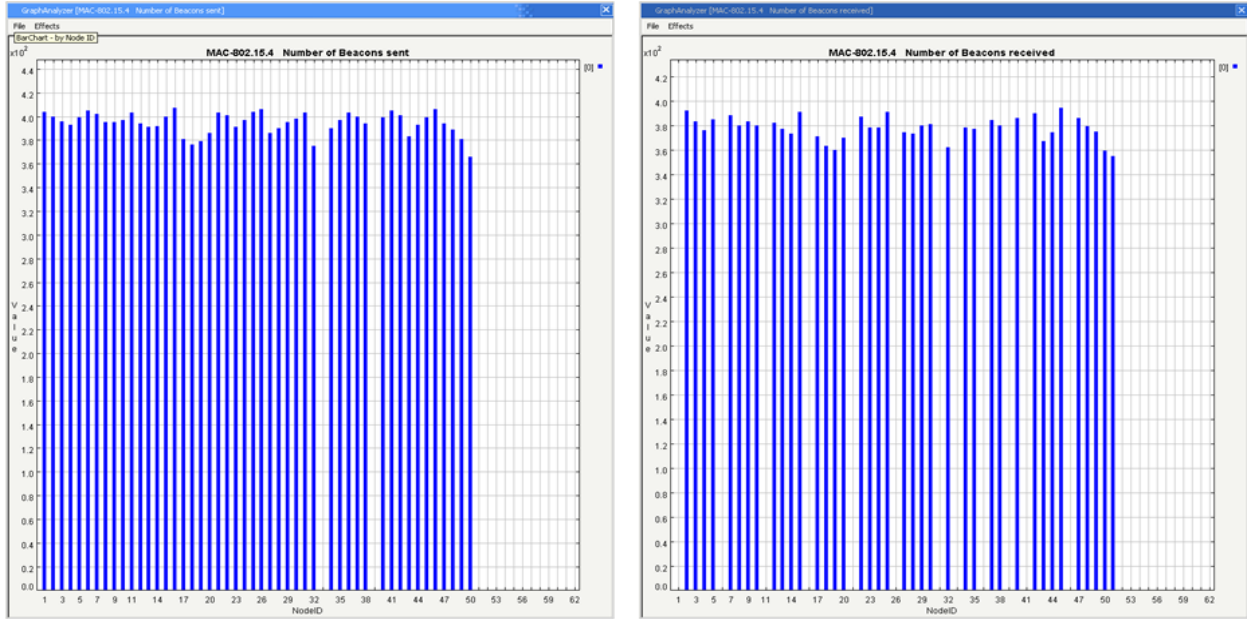


Figure 4.3 Number of beacon frames sent and received in QualNet

Figure 4.3 shows the number of beacon frames sent and received for this QualNet simulation scenario. The nodes that have not received beacon frames are the PAN coordinators (nodes 1, 6, 11, ..., 46) and nodes 33 and 39. Since nodes 33 and 39 have not received any beacons, they are unaware of networks in their neighborhood and thus cannot associate with their network. This lack of connectivity in turn prevents them from forwarding beacon frames.

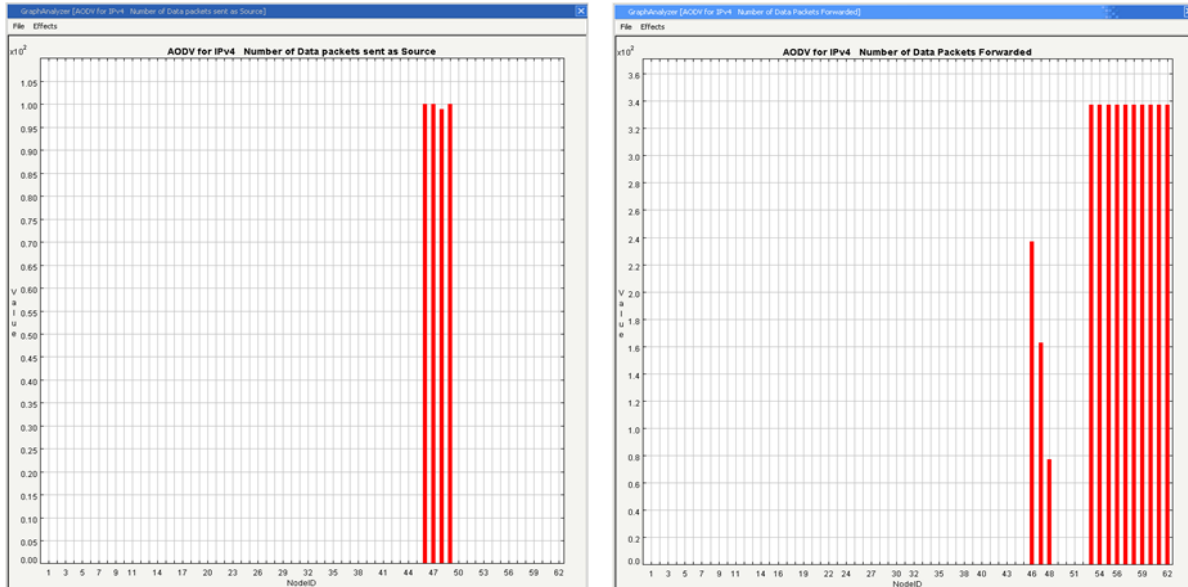


Figure 4.4 Number of data packets sent and received in QualNet

Since the CBR traffic are being generated by the sensors in the last WPAN, the failure of nodes 33 and 39 to join the network does not have any impact on this simulation. However, it does indicate that packet errors can be crucial for network discovery and network entry.

Each sensor in the last WPAN generates a total of 100 data packets, resulting in a sum total of 500 data packets to be expected at the data sink, but only 400 packets have been sent as shown in Figure 4.4 (left). All packets from node 50 have been dropped due to route failure. Figure 4.4 (right) illustrates the number of packets forwarded at each node. The number of packets at each WPAN node within the last PAN group increases at each hop because the node is a data source, generating its own packets, as well as forwarding packets from its child nodes. Once the packets enter the top-tier network (nodes 53 to 62), the packets are forwarded to the destination (node 52).

4.2.3 OPNET

We also wanted to test our multi-layer multi-hop wireless sensor network strategy in OPNET. We tried to set up a simulation as shown in Figure 4.5. Here, all Wi-Fi devices are located in the top row of nodes whereas each PAN coordinator is placed in the second row. Each Wi-Fi chipset and ZigBee PAN coordinator is directly connected to the other. However, after completing this configuration we discovered that OPNET's ZigBee module is implemented as its own stand-alone module and does not interoperate with other models in OPNET. Therefore, any attempt to start the simulation scenario failed.

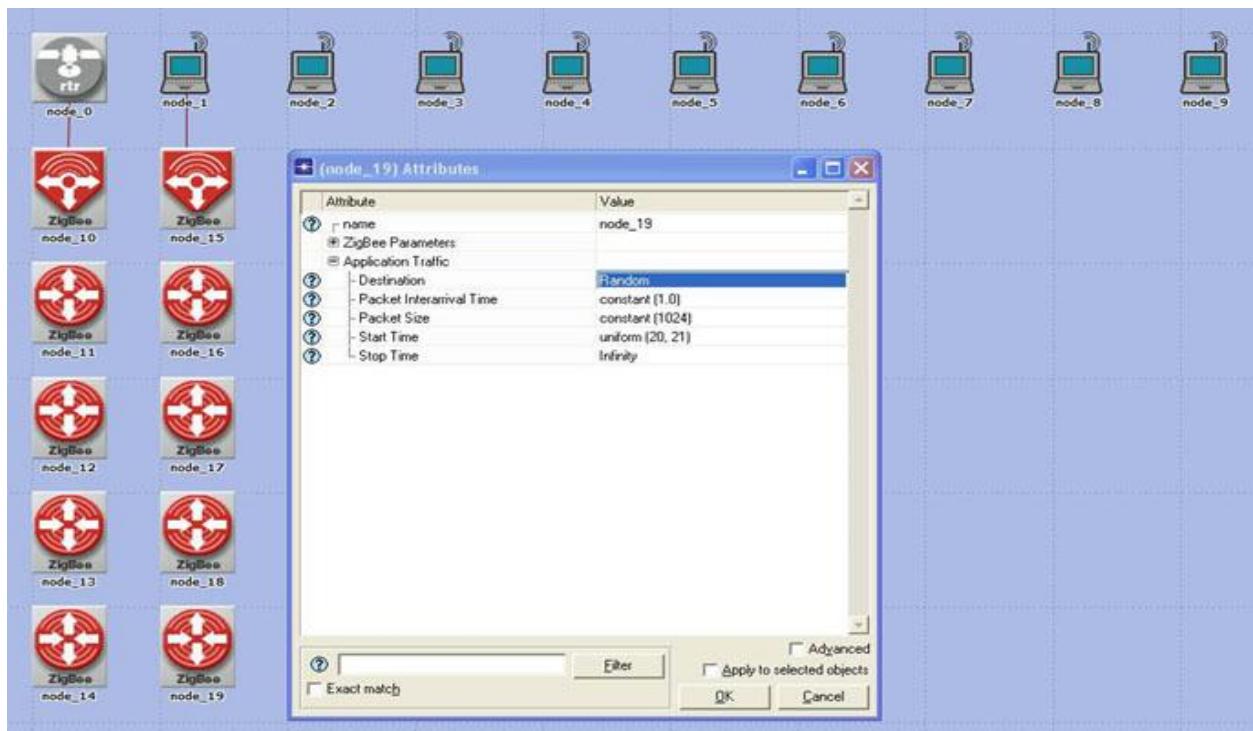


Figure 4.5 Multi-layer multi-hop wireless sensor network in OPNET

4.2.4 NS-2

Unlike OPNET, ns-2 supports interoperability between ZigBee and other technologies, such as 802.11b. Thus, it seemed that we can have both IEEE 802.11b devices and IEEE 802.15.4 devices running in the same simulation. Unfortunately, the original ns-2 node structure allows us to configure only one interface per node. This leads to a simulation configuration problem at the PAN coordinator which is intended to be a gateway to a Wi-Fi network and thus requires at least two interfaces: one for 802.15.4 and another for either 802.3 or 802.11b. There are two potential solutions for this problem. Firstly, we may opt to add a new node model to ns-2 in order to support multiple interfaces and also routing between interfaces. Secondly, ns-2 provides its own workaround for simulation that consists of wired and wireless networks, called wired-cum-wireless network. In this simulation, we used the second solution to quickly validate our proposed approach.

Figure 4.6 shows the achieved number of beacon frames sent, received, and dropped in our ns-2 simulation. The nodes 0-9 are the upper-layer Wi-Fi elementary nodes and therefore do not transmit beacon frames. Nodes 10, 15, 20, ..., and 55 are PAN coordinators that start by generating beacon frames. It takes less than 20 seconds to get all nodes synchronized, which is significantly less than a long single chain scenario required (130 seconds).

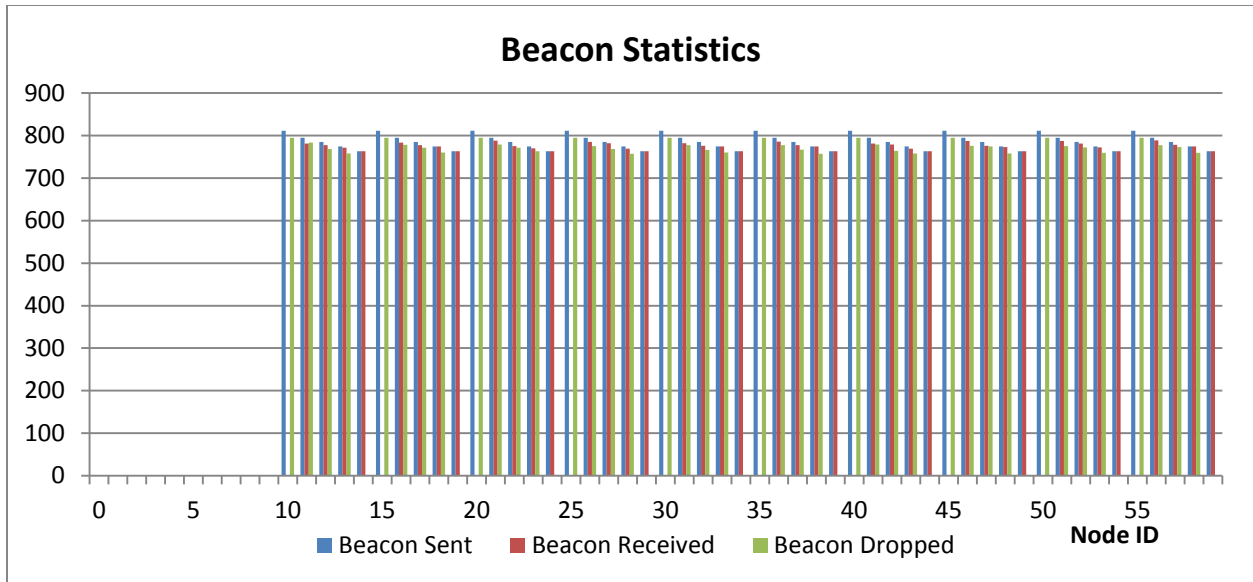


Figure 4.6 Number of beacon frames sent, received, and dropped in ns-2

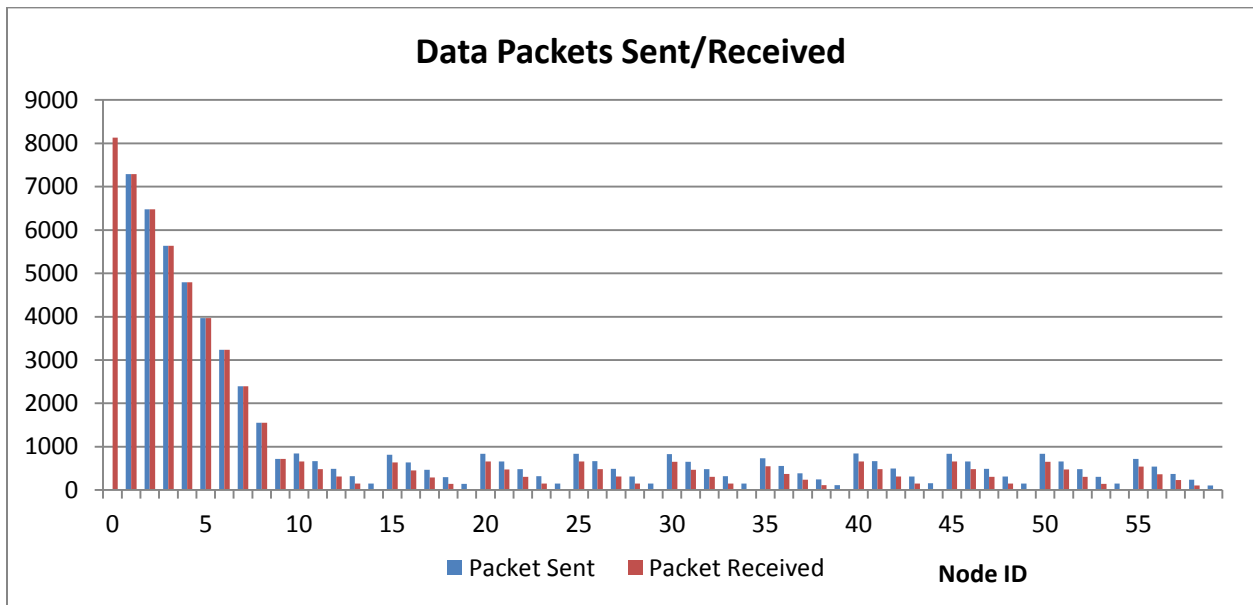


Figure 4.7 Number of data packets sent and received in ns-2

After synchronization, all sensors start transmitting data packets at 1 packet per second to the sink node (node 0). The simulation duration is 200 seconds, so we can expect each data source sensor node to send 180 packets. The intermediate nodes are responsible for forwarding

packets to their neighbors. Thus, each PAN coordinator should ideally have forwarded 900 packets to the data sink via the Wi-Fi top-tier network. Similarly, the Wi-Fi backhaul (nodes 0-9) aggregates more data with increasing number of traversed hops. At the simulation's conclusion we received 8,131 data packets successfully at the data sink node. In other words, 869 packets out of the total 9000 packets were lost. After careful tracing of the packet flow, we could determine that this occurred due to incomplete route discovery at the beginning of the simulation. Figure 4.7 shows the total number of data packets sent and received for each node in our ns-2 simulation.

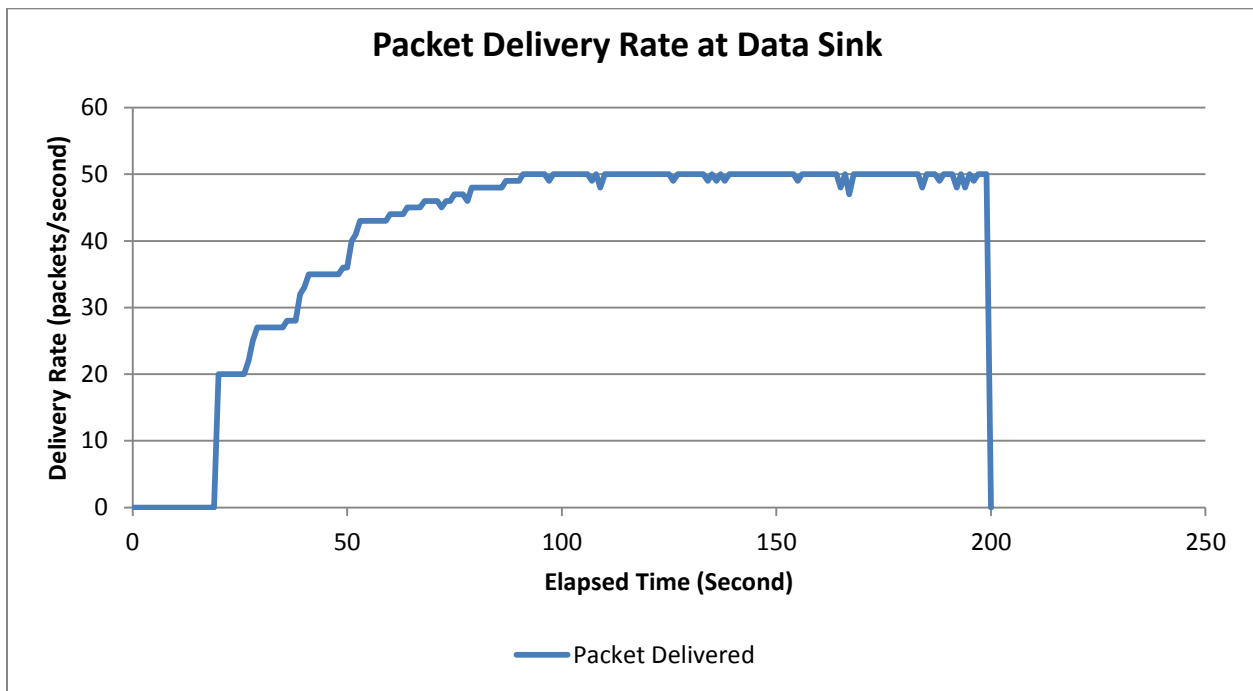


Figure 4.8 Number of packets delivered at destination in each second

Figure 4.8, which shows the delivery rate at the sink node in packets/second, highlights the packet loss at the beginning of the simulation. Note that in our simulation, traffic sources begin generating data at the 20th second. At the beginning of our simulation, only the first two

nodes in each PAN, the PAN coordinator and the ZigBee router that directly associates with it, have a known destination. All other nodes still have to establish route information. Thus, only the packets sent from these two nodes in each PAN are correctly delivered to the destination whereas the rest of the sensor nodes in each PAN will require additional time for finding the destination route. Once that is accomplished, all sensor nodes can successfully deliver packets to the destination.

4.3 Energy Analysis of the proposed multi-tier multi-hop scheme

By adding a long-range communication module onto the wireless sensor nodes—for example, using a Wi-Fi transceiver chipset—we also increase the energy requirements of the sensor nodes. Even considering that not every single sensor node will actually power up its Wi-Fi module (only one out of every 10 or so, depending on the number of nodes the long-range Wi-Fi link can bridge), there is still a net increase in energy-consuming elements in the network.

Therefore, to further analyze the feasibility of the proposed schemes we also studied the energy budget of an entire freight train's wireless network.

The basic assumptions of our theoretical energy budget analysis are as follows:

- 100 freight trains, one sensor per freight train
- Sensor nodes are arranged in a clear chain topology
- Sensor data traffic:
 - Each sensor generates a new reading once per second, resulting in a 70-byte data packet once per second.
 - In a WSN using traditional protocols, data is forwarded by each sensor along the chain of nodes, whereas in the multi-tier network, data is

forwarded towards the active Wi-Fi node in the neighborhood where all data is then forwarded farther using the Wi-Fi link.

- Sensor Node 100 is the destination node at the locomotive. All sensors are tasked with delivering their data to this node.

To evaluate the network lifetime we further assumed that each sensor is equipped with the same amount of initial energy. This is based on the following energy capacities of different energy storage technologies, shown in the following table.

Table 4.1 Battery Types and their average energy storage capacities

Battery Type	Avg. voltage During discharge	Milliamp hours (mAh)	Watt-hours (Wh)	Joules (J)
Alkaline	1.225	2122	2.60	9360
Carbon-zinc	1.1	591	0.65	2340
Nickel-Cadmium	1.2	1000	1.2	4320
NiMH	1.2	2100	2.52	9072
Lithium Ion	3.6	853	3.1	11050

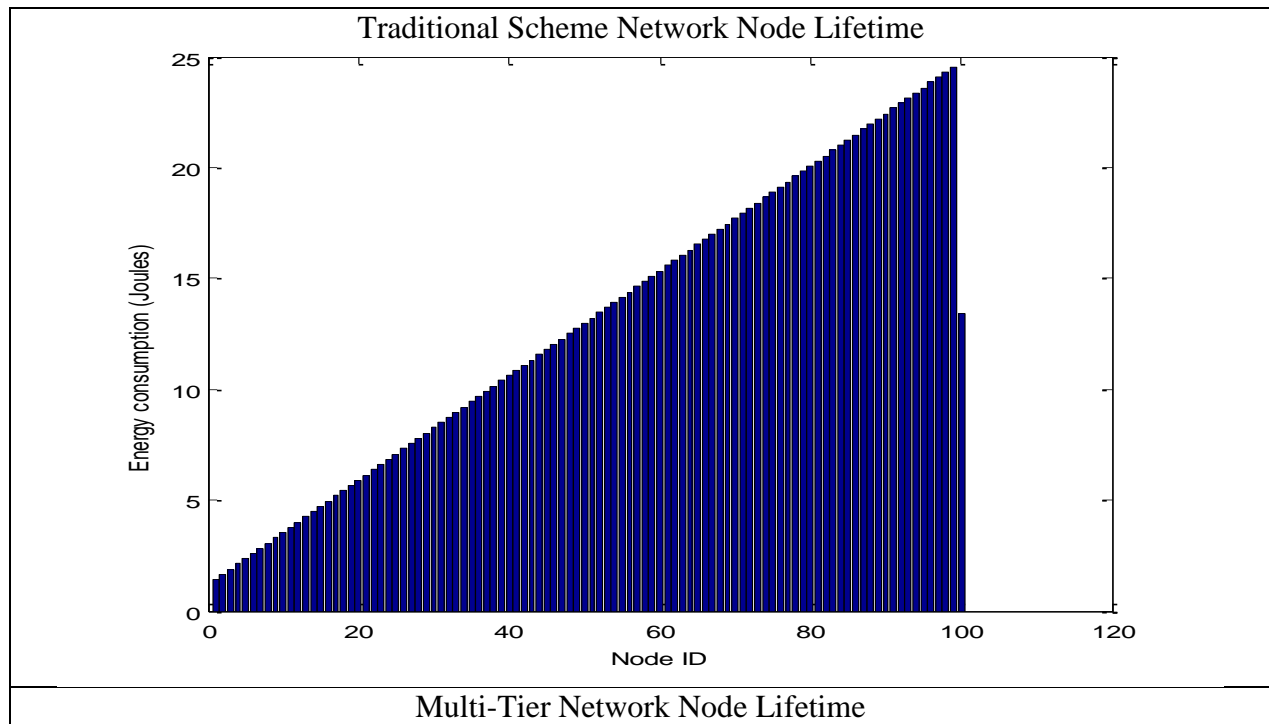
Based on these numbers, we chose to utilize a single battery with 10,000 joules of charge; this is approximately equivalent to a single AA battery.

Furthermore, we collected power consumption statistics from currently available ZigBee and Wi-Fi chipsets, shown in the following table.

Table 4.2 Zigbee and Wi-Fi Chipset comparison for power consumption

Wireless sensor node	Low-power Wi-Fi node
• RxPower = 56 mW	• RxPower = 40 mW
• TxPower = 52 mW	• TxPower = 360 mW
• IdlePower = 1.3 mW	• IdlePower = 40 mW
• SleepPower = 48 uW	• SleepPower = 36 uW
Texas Instrument CC2420	Roving Networks RN-111B

Given this data we could now calculate the energy consumption per node for the traditional approach and our proposed multi-tier approach to freight train WSNs. The results of both approaches are shown in figures 4.9 and 4.10.



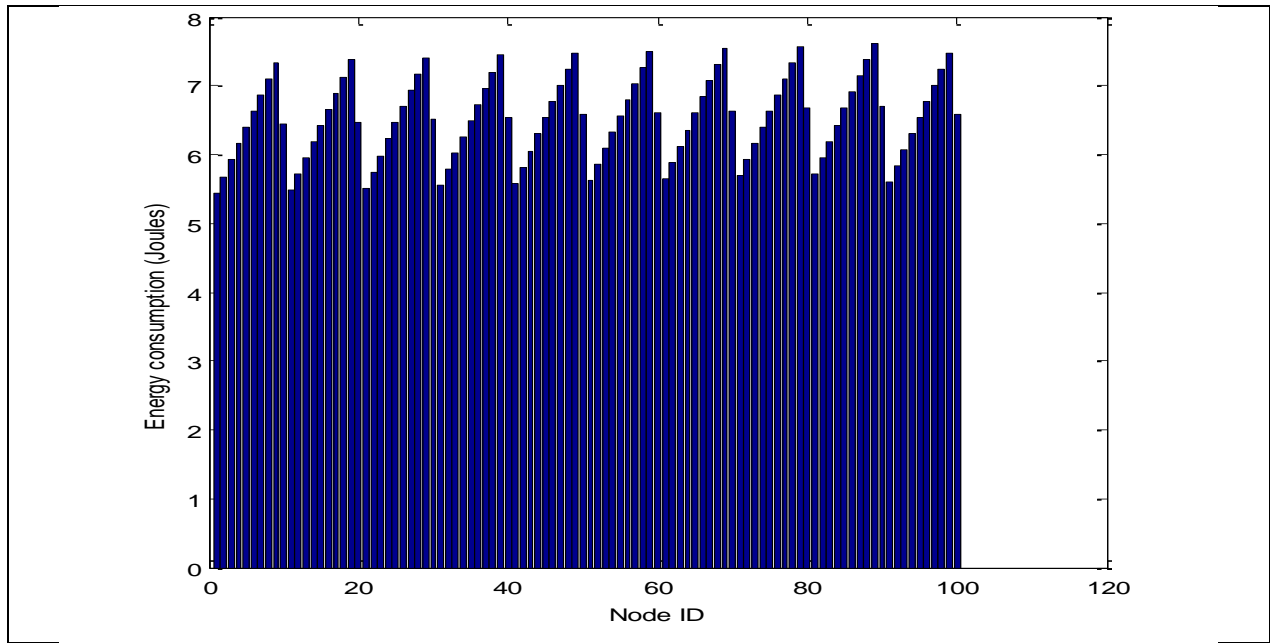
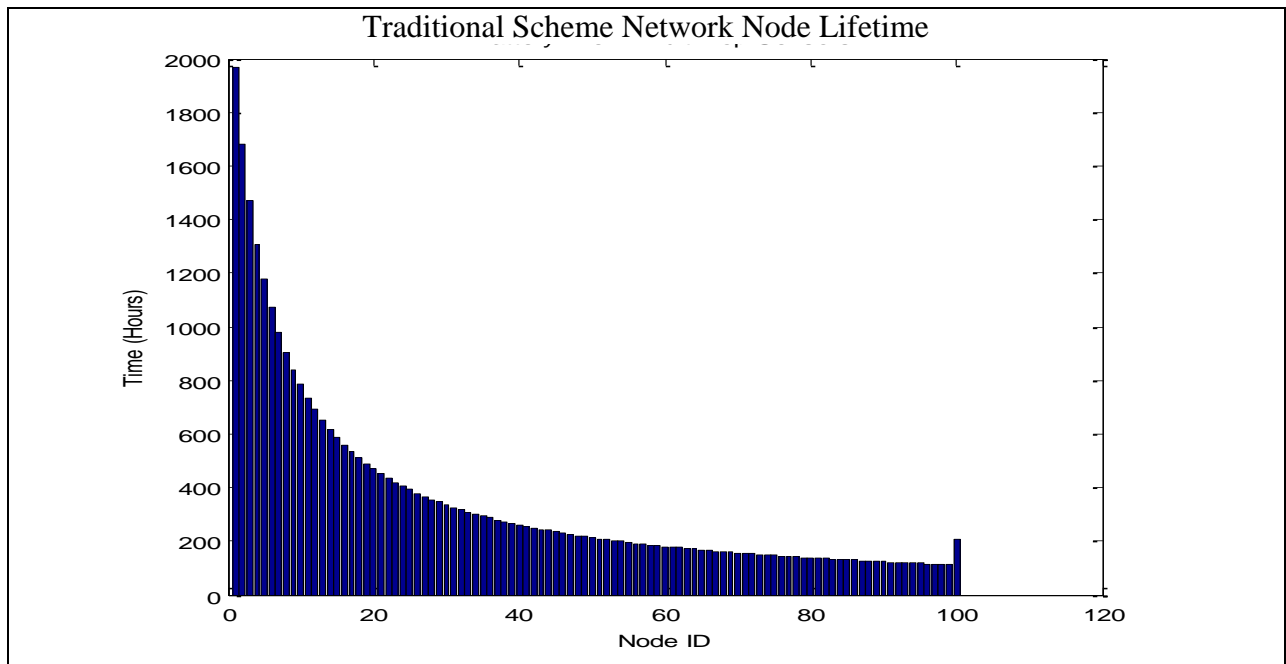


Figure 4.9 Energy consumption per node comparison

Based on these results and the given energy storage capacity per node we could also calculate the node lifetime:



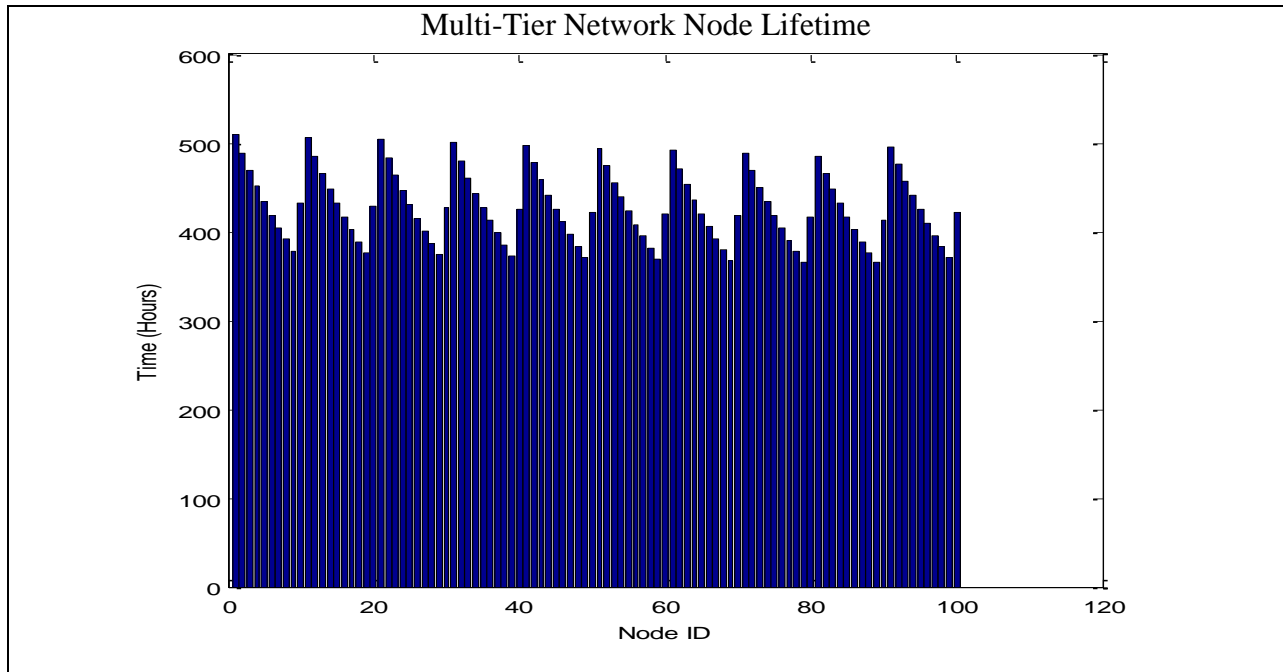


Figure 4.10 Network Lifetime comparison between traditional scheme and multi-tier networking

From the above results we can clearly see that some nodes have a longer lifetime in the traditional scheme than in the new multi-tier scheme. However, we define network lifetime as the time until the data delivery to the desired destination node fails. This is rooted in the core principle of WSNs as application-driven networks. If the application of the WSN can no longer be accomplished, the network is effectively inoperable.

Given that definition, we can find that in the traditional scheme the critical node 109, the direct neighbor of the data sink node, fails after **113.1 hours**, whereas the earliest failure that occurs in the multi-tier network takes places after **364.9 hours**. In other words, the multi-tier network scheme actually improves network lifetime by a factor of **more than 3 times**.

Chapter 5 Publications

Throughout the project we pursued publication of the work we performed and the results we obtained in the process. We strongly believe that in making our findings and insights into the simulation environments and our developed multi-tier approach to freight train wireless sensor networks available to other researchers in industry and academia, we can aid their work and at the same time inform others about the progress we made on this important research topic.

Currently, we have completed three publications. One of our articles [14] was published by ITS America, the Intelligent Transportation Society of America, and presented at their annual meeting in Houston, TX, in May of 2010. This paper was nominated by ITS America to also be submitted to the ITS World Congress to be held October 2010 in Busan, South Korea, and was accepted for publication [15].

Our third paper [16] was accepted to IEEE SENSORS to be presented there in November of 2010, and will focus on the multi-tier networking approach rather than the simulation work we performed and presented in the two ITS papers.

We are currently working on additional publications of our research work for the Transportation Research Board's Journal, the *Transportation Research Record*, and other related journals and conferences.

Chapter 6 Summary

This project focused on studying the characteristics of Wireless Sensor Networks onboard freight trains. In North America, freight railroad companies are searching for ways to improve their monitoring capabilities and fault detection of individual railcars. Currently, such faults can only be detected at wayside detectors, which are costly to implement, or when the train pulls into a yard.

Wayside detectors currently cover only a very small fraction of the North American railroad track network. Based on figures by the FRA and published in a study by Booz Allen Hamilton in 2006, the minimum initial cost per site for wayside detectors is \$250,000, with annual maintenance costs equaling a significant portion of that amount. Even with a significant build-out of wayside detector stations across North America, faults can still only be detected when the train passes such detector sites, with no monitoring provided while travelling between wayside detectors. As a result, neither approach is a feasible method of preventing loss of freight or accidents.

However, small battery operated wireless sensor nodes can easily be installed onboard freight railcars to monitor a variety of systems, from wheel imbalances and brake failures to refrigerator units, boxcar doors, and many more. Since the sensors are installed directly on the railcars, at the site of potential failures, monitoring can be provided in real-time, with immediate notification of the train operator and dispatch centers. This system has the potential to prevent most fault-related train accidents through early detection and alerting.

This study first evaluated the propagation characteristics of wireless sensor nodes deployed onboard railcars and found that placement of these nodes significantly impacts the radio wave propagation characteristics. This is further complicated by the materials used in

railcar construction and their design. We have shown with our results that roof-mounted antenna systems seem the most suitable for wireless communication between railcars. However, roof-mounted installation is not always appropriate, given the specific location of a monitored system component, such as a wheel. Therefore, the network structure needs to account for location and the potential communication distance of each node, which in turn drastically impacts the requirements upon the wireless communication protocols at the MAC and Routing layers.

Therefore, in our second research effort that comprises this project, we studied the performance of ZigBee, a communication protocol stack commonly used in traditional wireless sensor networks, and found it to be inadequate for the particular requirements of freight train wireless sensor networks.

We then proposed an alternative approach and studied its performance in an effort to overcome the limitations of ZigBee for freight car WSNs. Our proposed solution leverages a multi-tiered approach to improve upon the long-chain topology found with the traditional approach. We utilize long-range wireless radios added to the wireless sensors to provide a long-range communication link that “jumps” over entire segments of wireless nodes.

The proposed solution has been shown in our simulation study to be very promising in overcoming the problems associated with standard ZigBee for railroad wireless sensor networks. In particular, our approach represents a significant reduction in maximum hop distance between traffic source and destination by leveraging a long-range wireless technology such as Wi-Fi as an overlay communication tier for interconnecting subsets of wireless sensor nodes, effectively converting the chain topology into a hierarchical structure.

However, the currently available simulation tools are incomplete in their implementation of the ZigBee communication protocol. Our team therefore invested significant additional

resources into completing the implementation of the NS-2 ZigBee simulation environment and our multi-tier networking technology.

We found that our design provides significant performance improvements over the traditional approach, as well as significantly improved energy efficiency and network lifetime.

Finally, we would like to thank Union Pacific for their generous support of our research throughout the entire project. UP provided technical expertise in railcar monitoring, sensor platforms for lab testing, and an open ear for all of our questions. We always cherish the close collaboration of our team here at TEL with the people at Union Pacific.

The results produced by this research project will have a significant impact on the direction and future work by the railroads in North America, including Union Pacific. The insights into the propagation characteristics of freight train wireless sensor networks is of great benefit to the railroad engineers that will design and implement these networks on freight trains nationwide, making freight railroad operation safer, more secure, and more efficient.

References

- [1] University of Nebraska-Lincoln. [Online]. www.unl.edu
- [2] Advanced Telecommunications Engineering Laboratory at UNL. [Online]. <http://www.tel.unl.edu>
- [3] Union Pacific. Union Pacific. [Online]. <http://www.up.com>
- [4] Mid-America Transportation Center. MATC Website. [Online]. <http://matc.unl.edu>
- [5] Computer Simulation Technology, Inc. CST Corporate Website. [Online]. <http://www.cst.com>
- [6] ZigBee Alliance. ZigBee Alliance Website. [Online]. <http://www.zigbee.org>
- [7] IEEE 802.15 WPAN Task Group 4, "Part 15.4: Wireless Medium Access Control (MAC) and Physical Layer (PHY) Specifications for Low-Rate Wireless Personal Area Networks (WPANs)," 2009.
- [8] QualNet Network Simulator. [Online]. www.scalable-networks.com
- [9] OPNET Network Simulator. [Online]. www.OPNET.com
- [10] NS-2: The Open Source Network Simulator. [Online]. www.isi.edu/nsnam/ns/
- [11] Crossbow Technology, Inc. Corporate Website. [Online]. <http://www.xbow.com>
- [12] Arch Rock. Corporate Website. [Online]. <http://www.archrock.com/>
- [13] Azimuth Systems, Inc. ACE-400WB Website. [Online]. <http://www.azimuthsystems.com/platforms-channel-400wb.htm>
- [14] Puttipong Mahasukhon et al., "Multi-Tier Multi-Hop Routing in Large-Scale Wireless Sensor Networks for Freight-Train Monitoring," *ITS America Annual Meeting*, May 2010.
- [15] Puttipong Mahasukhon et al., "Multi-Tier Multi-Hop Routing in Large-Scale Wireless Sensor Networks for Freight Train Monitoring," *Proceedings of the ITS World Congress*, October 2010.
- [16] Puttipong Mahasukhon et al., "Multi-Tier Multi-Hop Routing in Large-Scale Wireless Sensor Networks for Real-Time Monitoring," *Proceedings, IEEE Sensors*, November 2010.
- [17] Federal Railroad Administration. [Online]. www.fra.dot.gov
- [18] Peter Kiewit Institute. [Online]. <http://www.pki.nebraska.edu>

Appendix

Appendix A: Additional Results from EM-Field Study of RF Propagation Characteristics

This section includes additional results collected as part of our comprehensive evaluation of physical layer RF propagation characteristics for different types of railcars and antenna placements.

Each data set includes the antenna placement and railcar configuration picture, the resulting farfield antenna pattern picture, as well as the E-Field visualization.

The included results are for:

- Roof mounted
 - Tanker car
- Side-mounted antenna
 - Flat car
 - Tanker car
 - Hopper car
- Undercarriage-mounted antenna
 - Flat car
 - Tanker car
 - Hopper car
- Passing trains
 - Flat car
 - Tanker car
 - Hopper car
- Train segment
 - Flat car
 - Tanker car
 - Hopper car

Figure A.1. Tanker car: roof-mounted antenna

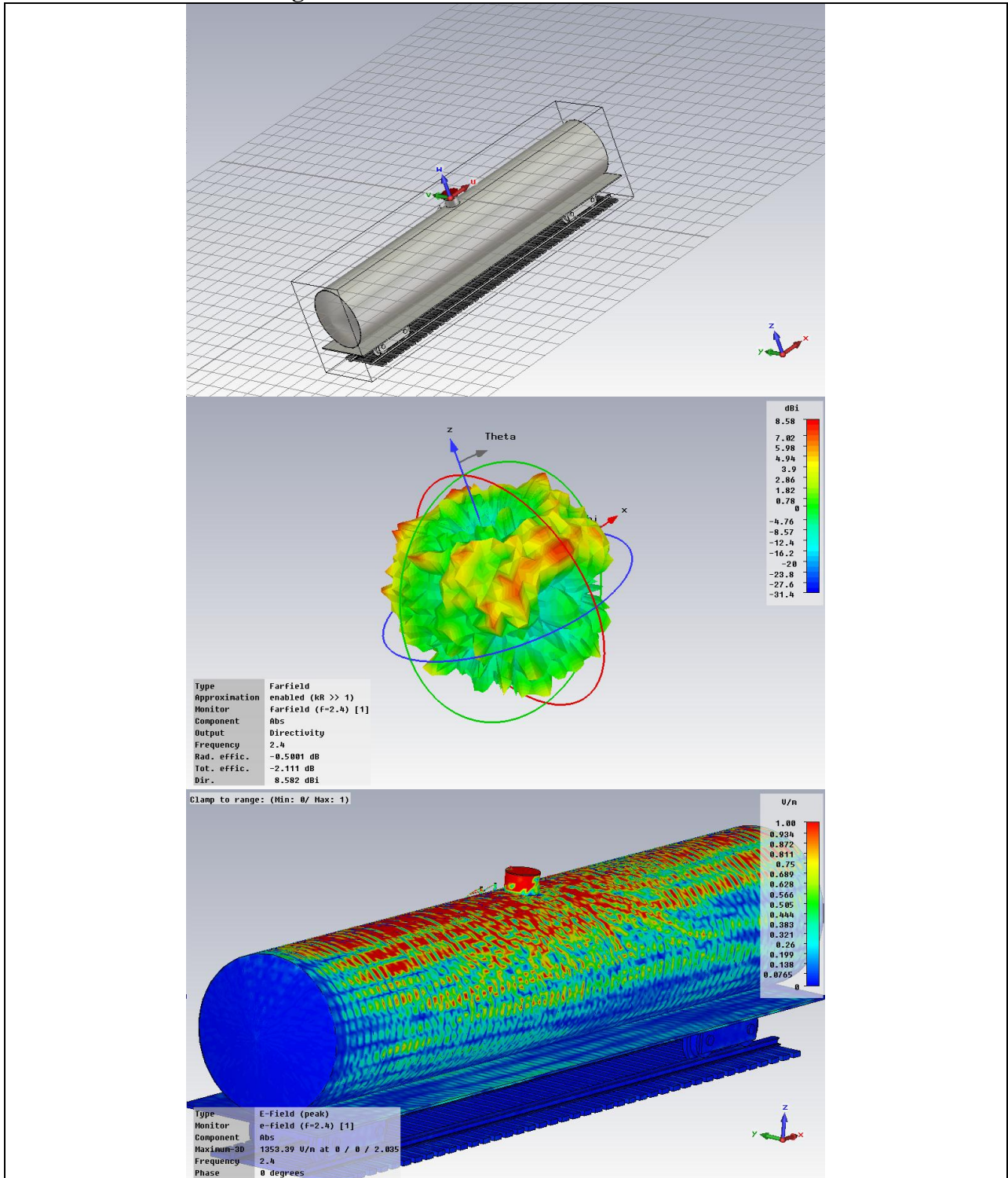


Figure A.2. Flat car: side-mounted antenna

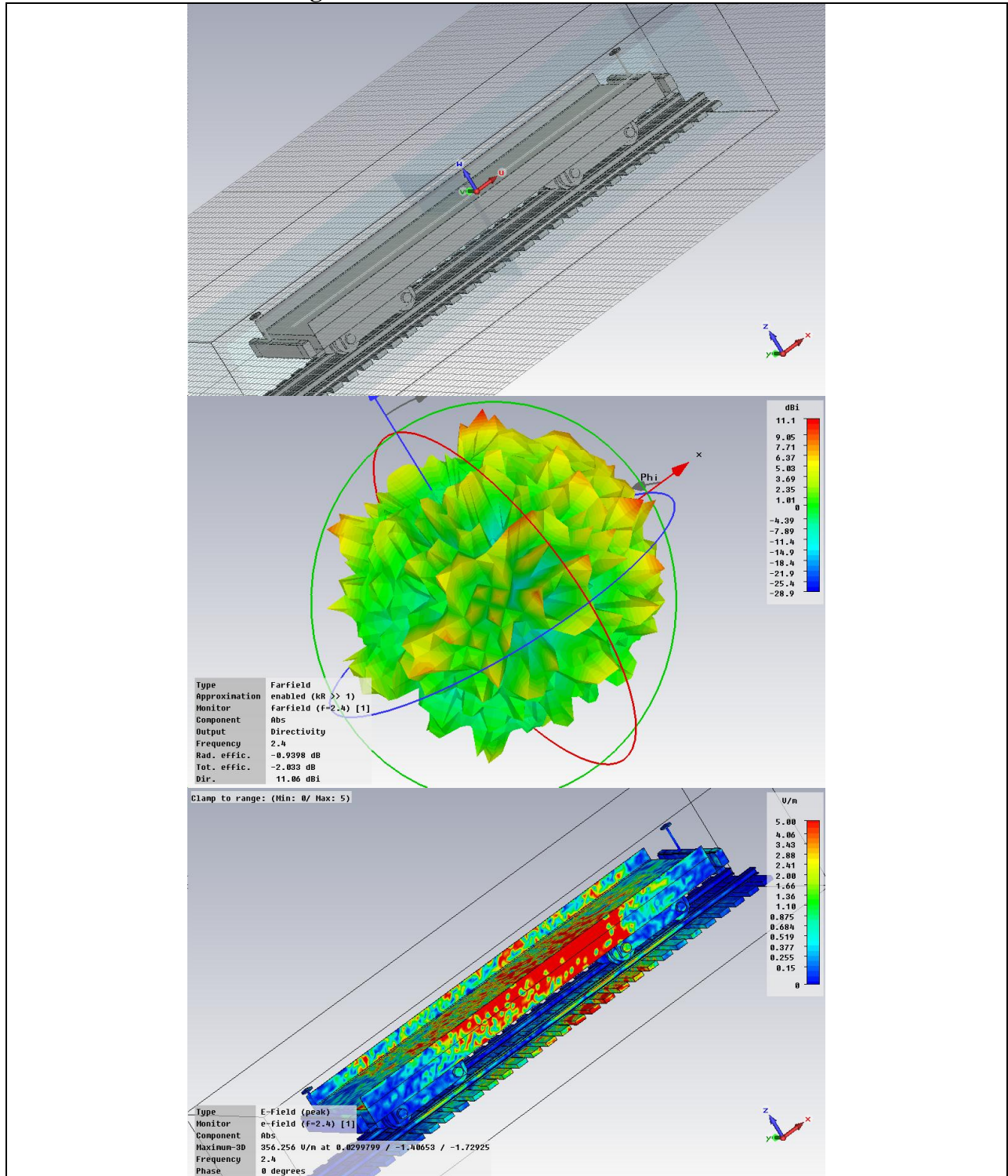


Figure A.3. Tank car: side-mounted antenna

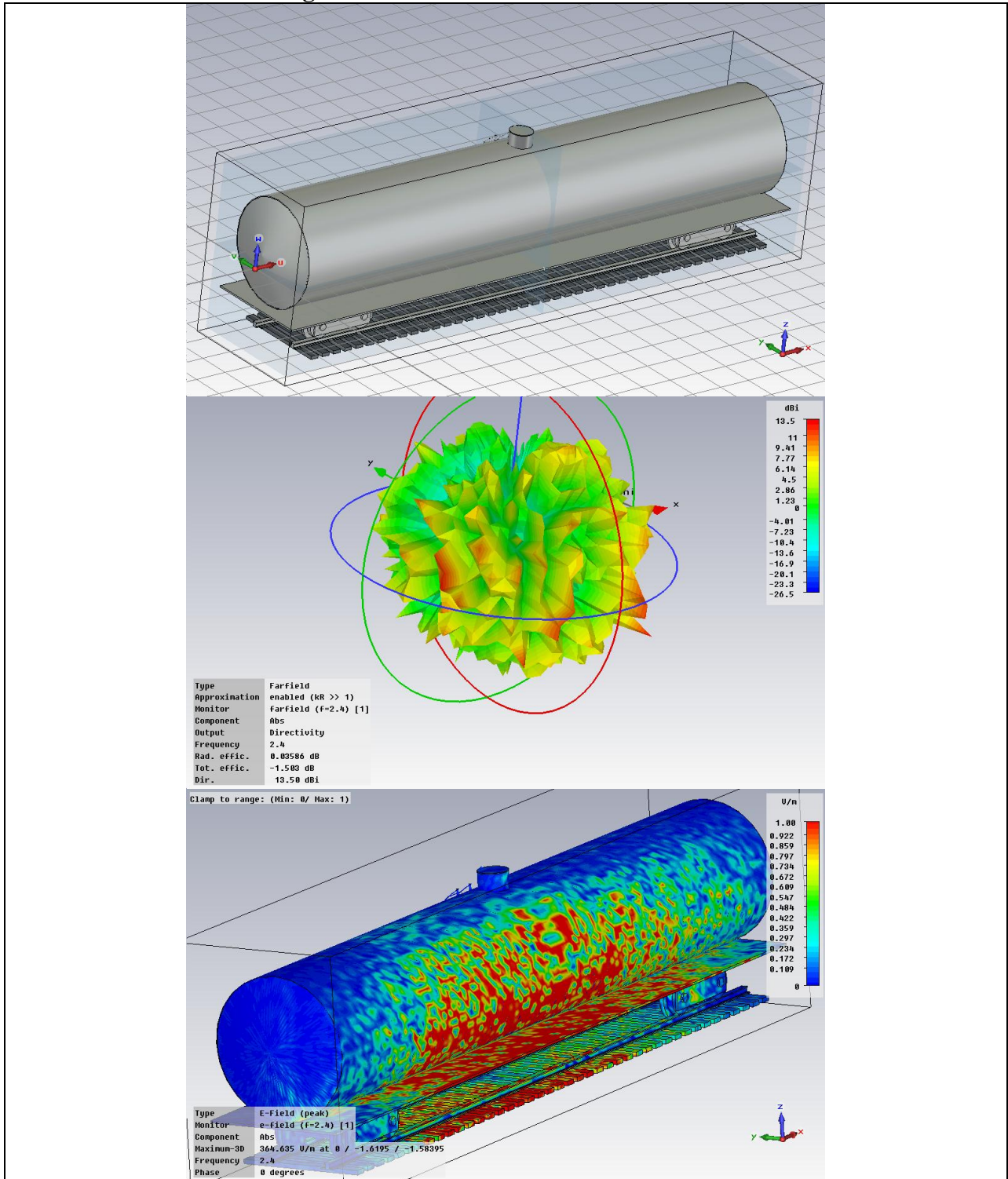


Figure A.4. Hopper car: side-mounted antenna

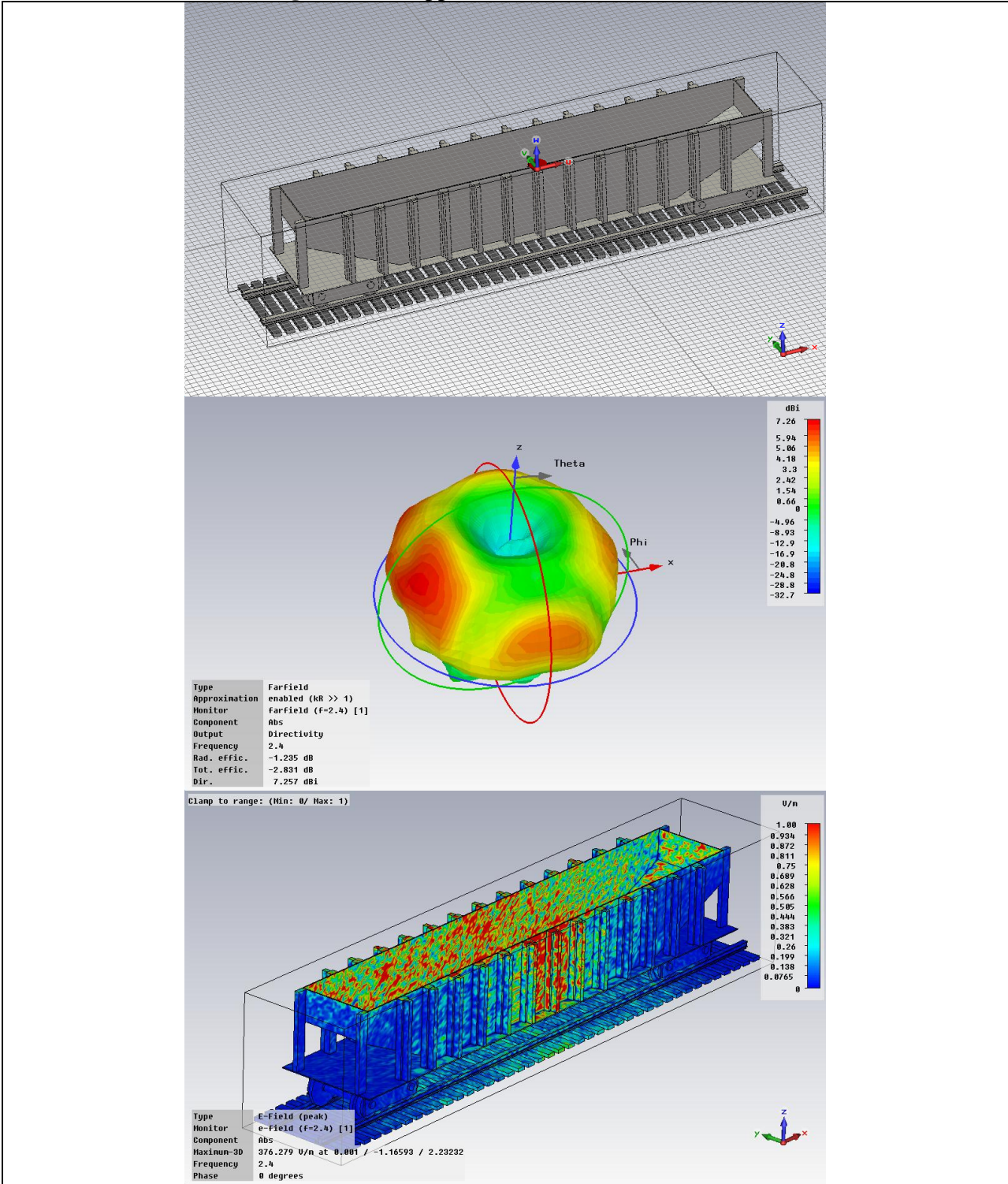


Figure A.5. Flat car: undercarriage-mounted antenna

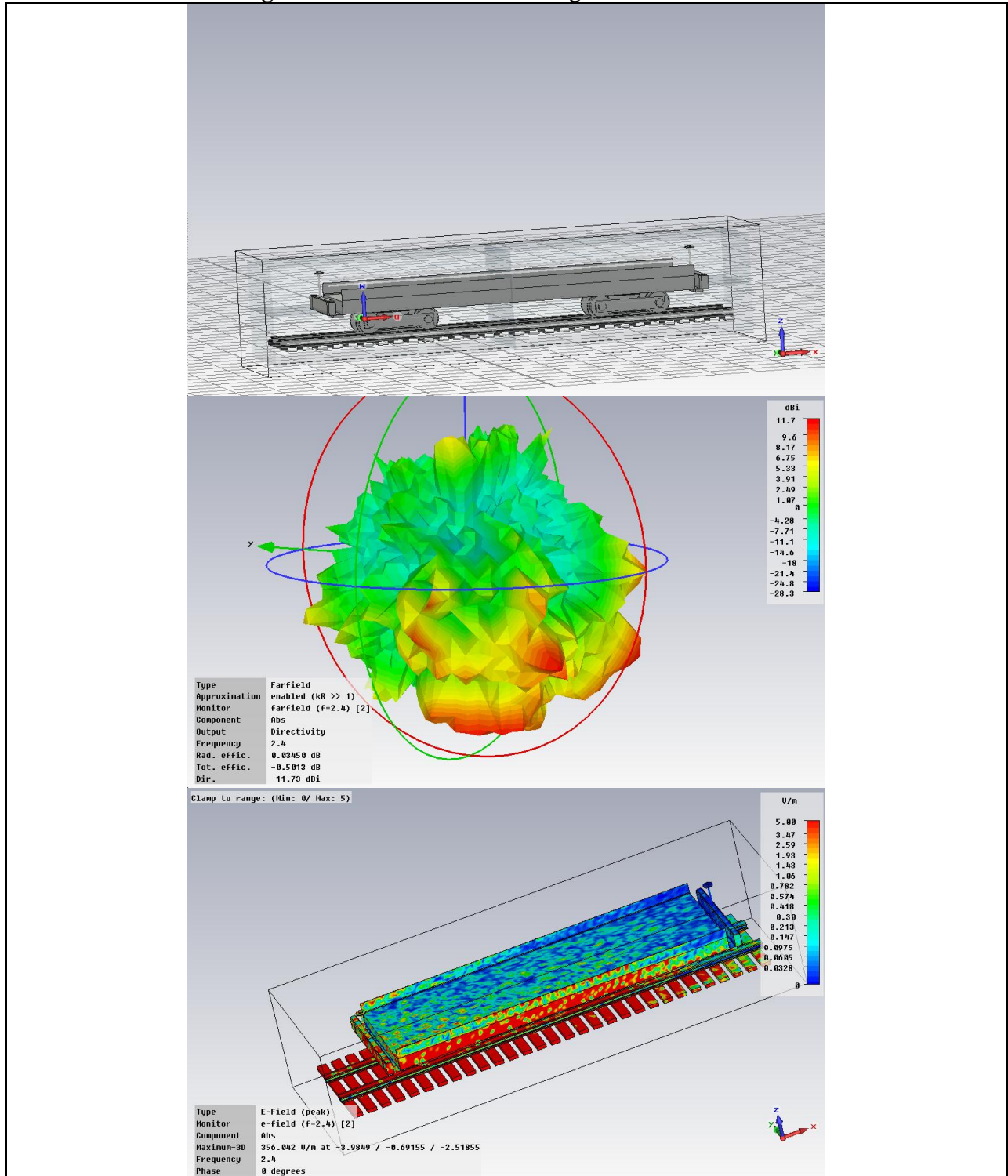


Figure A.6. Tank car: undercarriage-mounted antenna

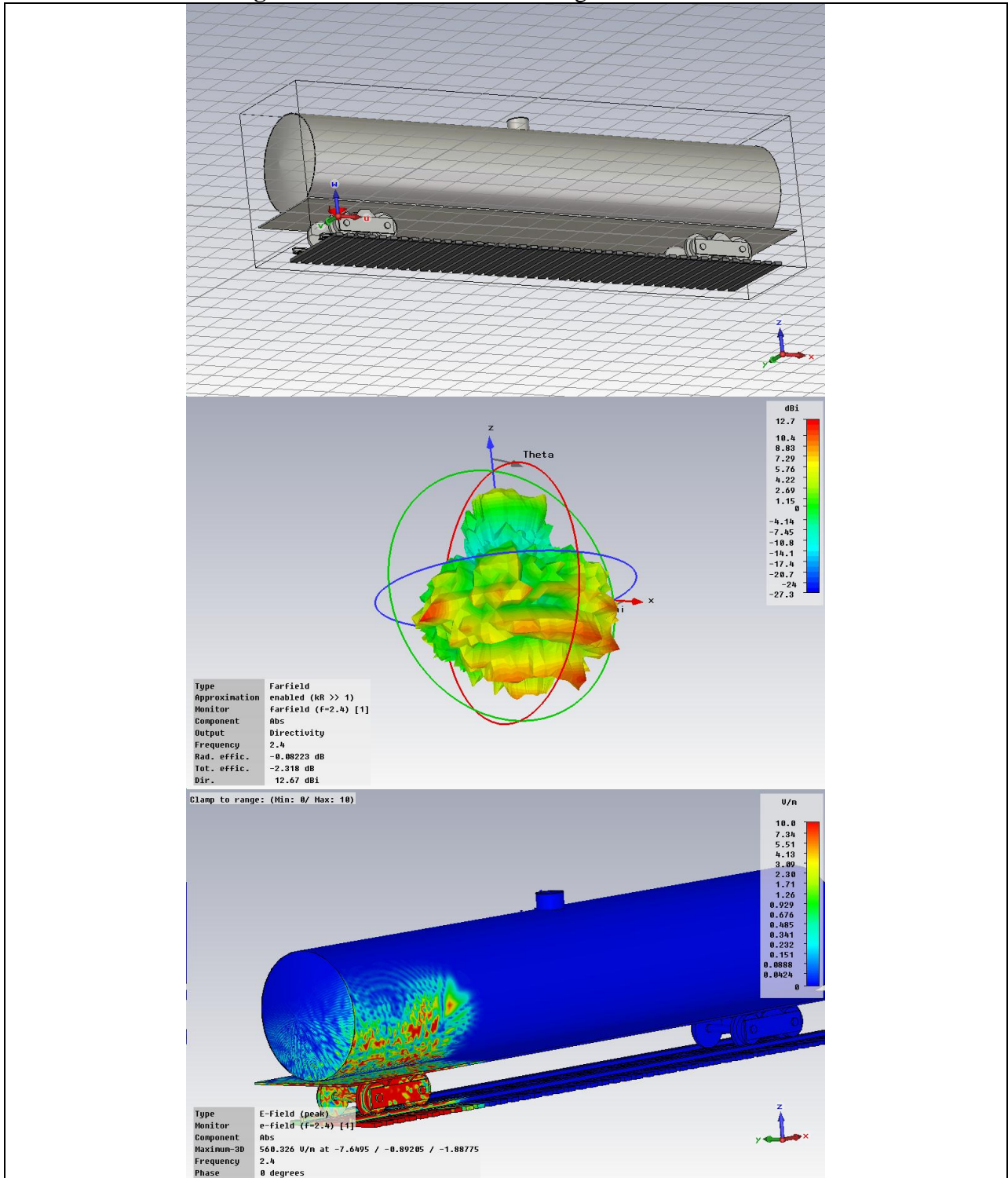


Figure A.7. Hopper car: undercarriage-mounted antenna

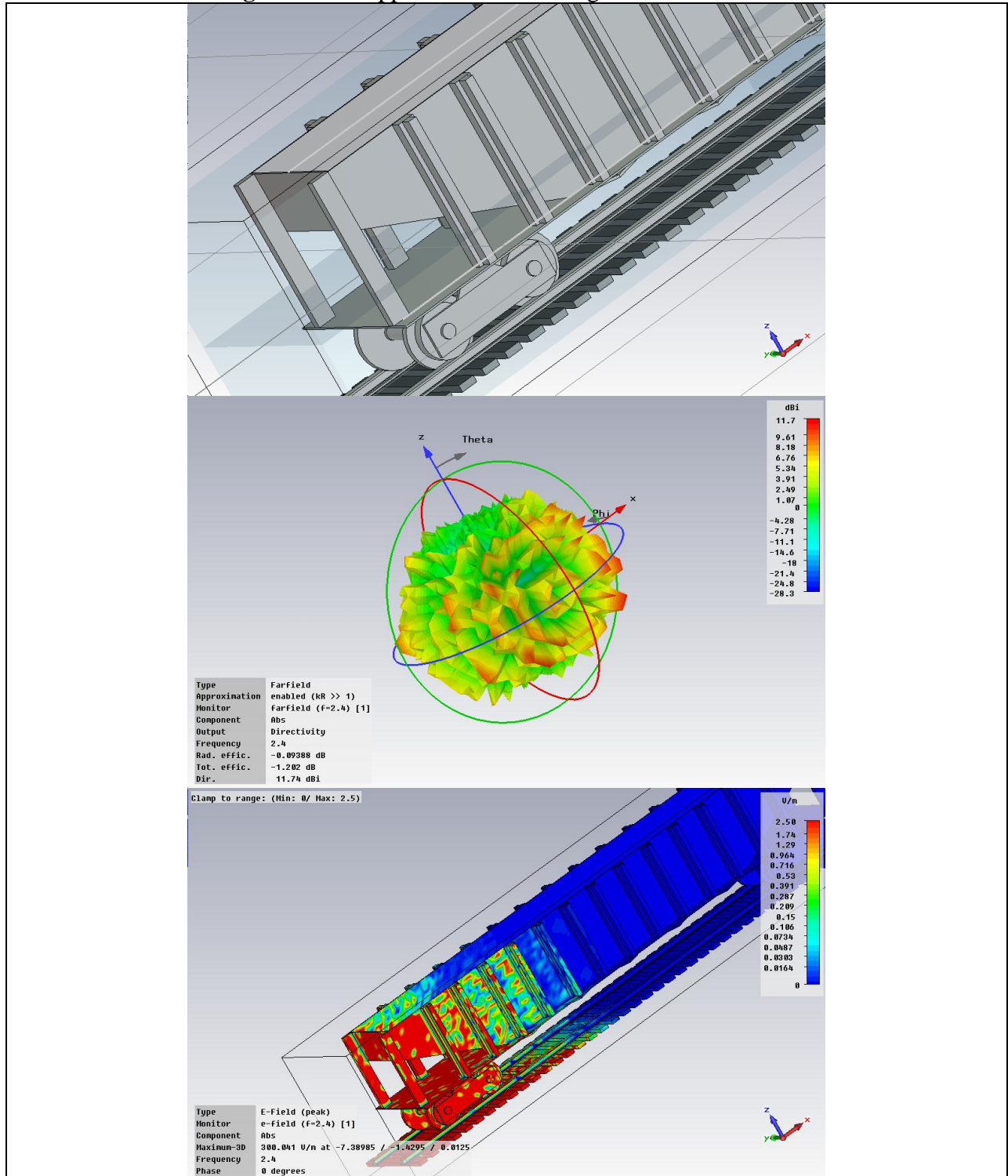


Figure A.8. Flat car: passing train

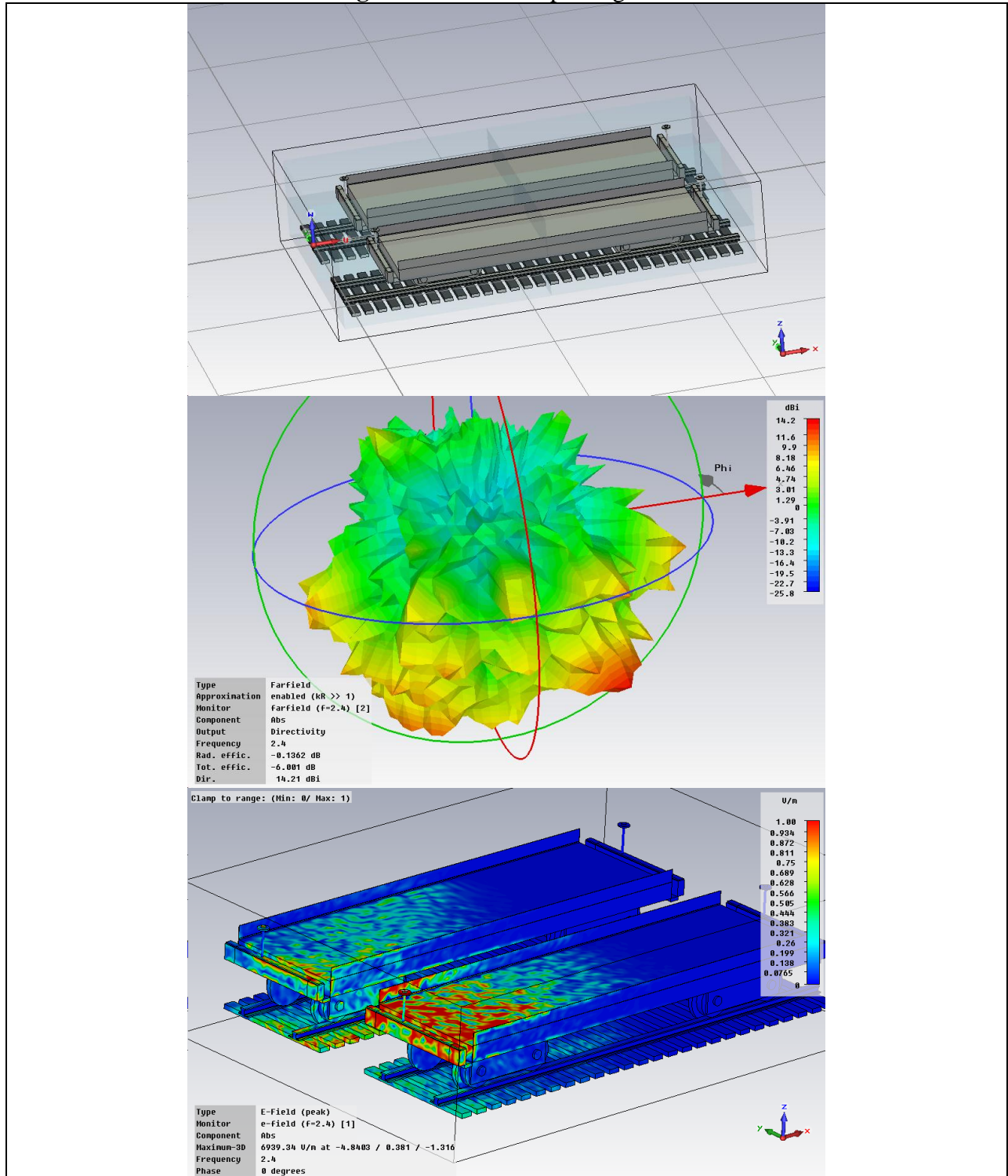


Figure A.9. Tanker car: passing train

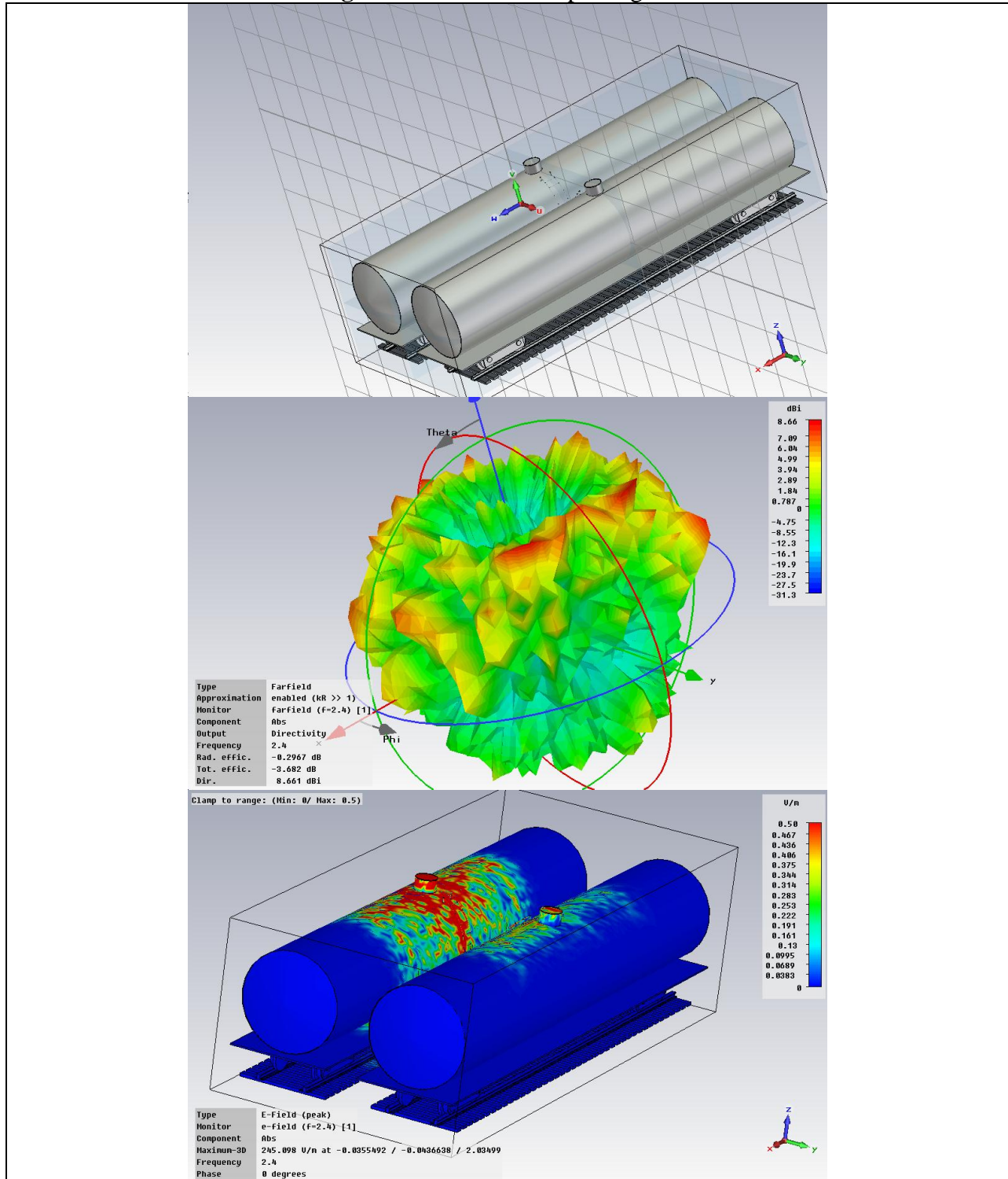


Figure A.10. Hopper car: passing train

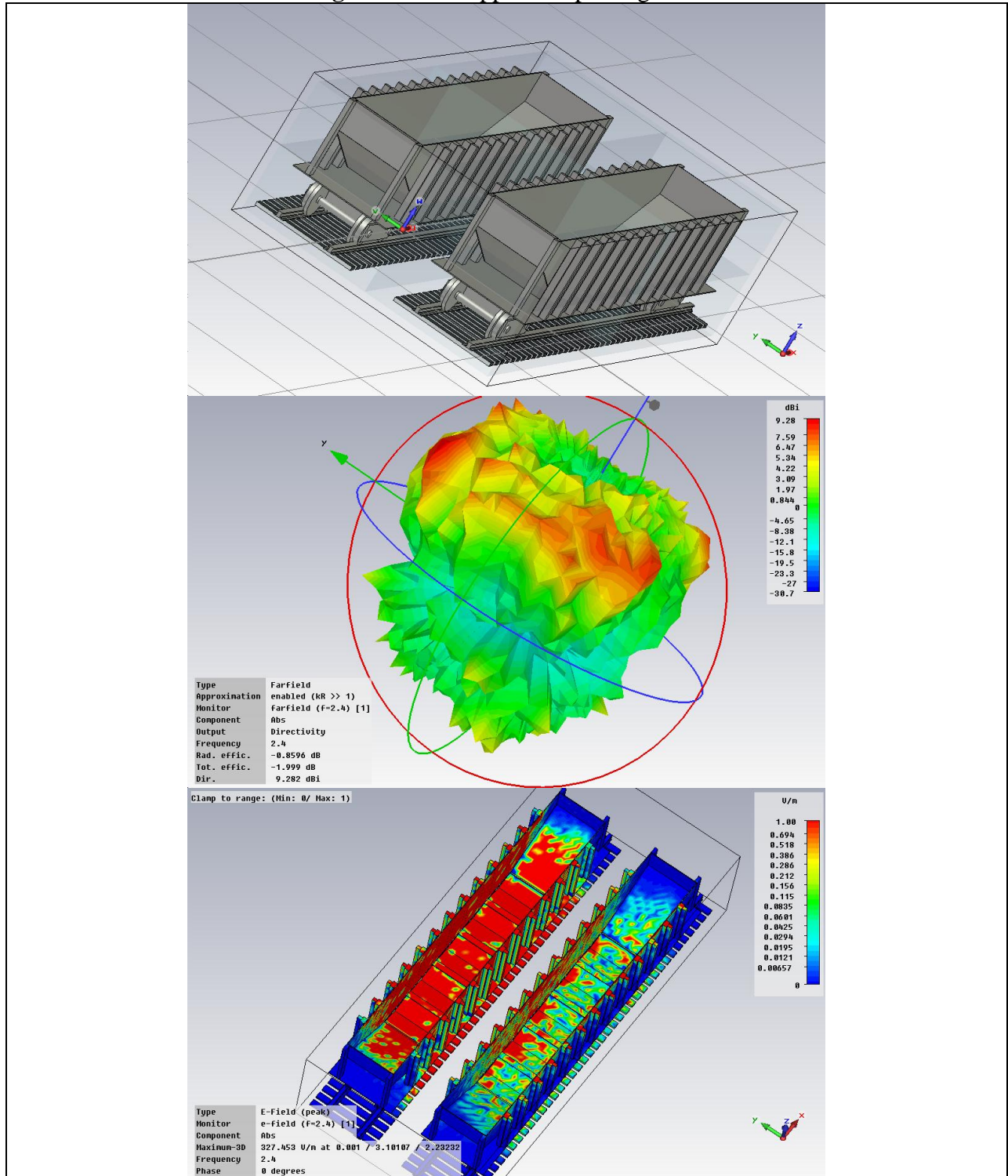


Figure A.11. Flat car: train segment

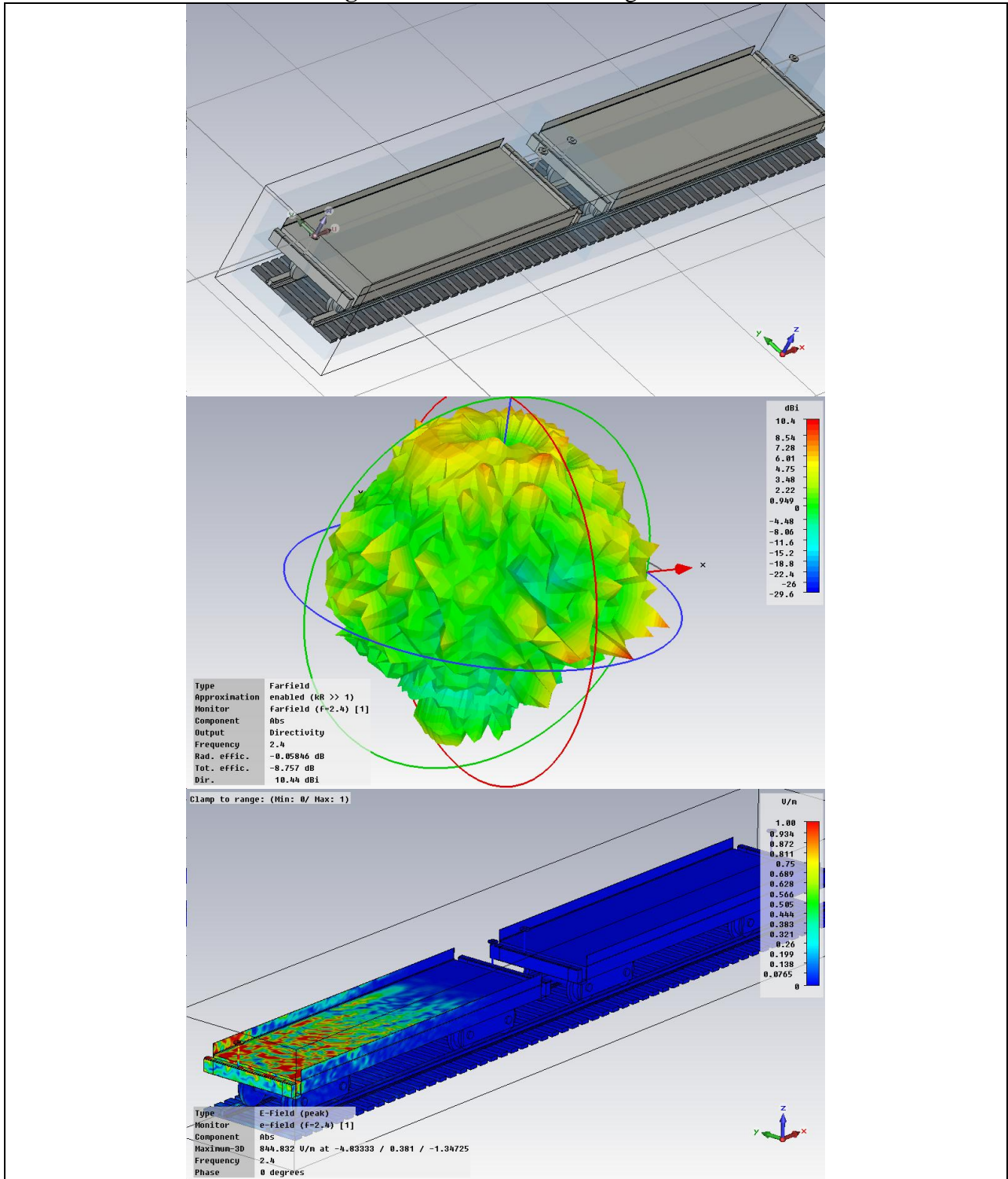


Figure A.12. Tanker car: train segment

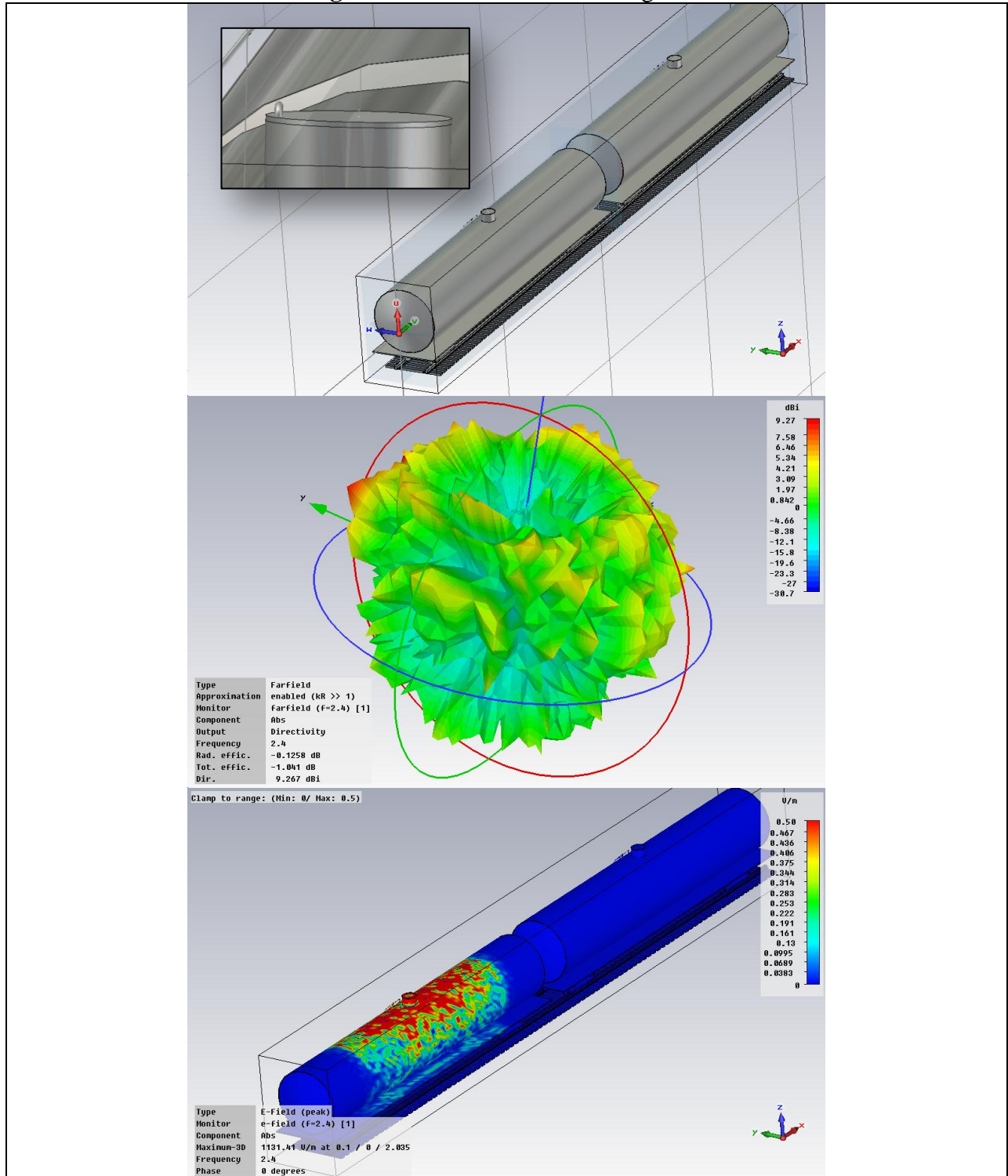


Figure A.13. Hopper car: train segment

